A silicon based polarimeter for pEDM searches

James Gooding

E. Vilella-Figueras, G. Casse, N. Rompotis
T. Bowcock, J. Vossebeld, J. Price

Proton EDM

- Overview and experimental method

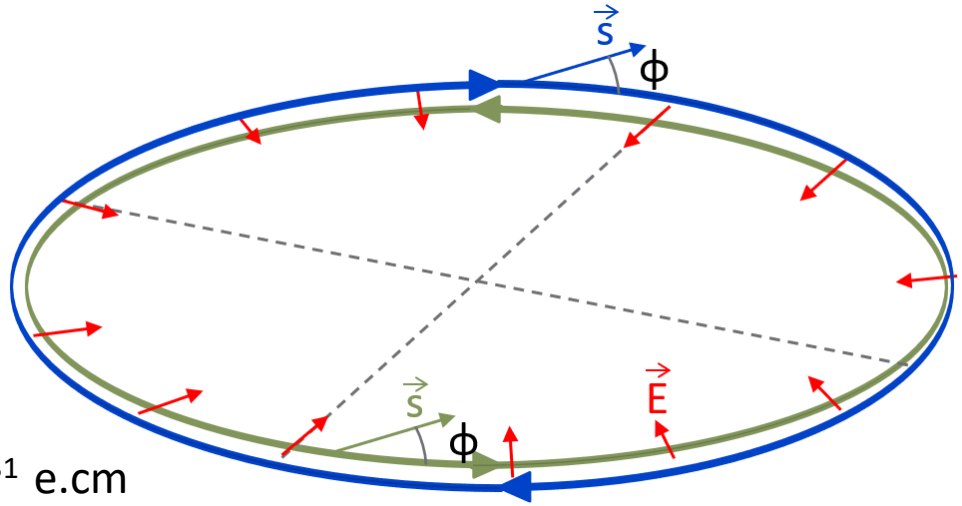

- Matter/antimatter asymmetry → CP violation → permanent EDM
- An EDM is caused by separation of permanent charges inside a particle
- Closely connected to spin of the particle which is influenced by E & B fields
- The standard model predicts proton (and neutron) EDM's at the level of 10^{-31} e.cm
- Some BSM predict nucleon EDM's in the range 10^{-24} - 10^{-28} e.cm range
- Neutron EDM limit: d_n is $(0.0 \pm 1.1)\times10^{-26}$ e.cm

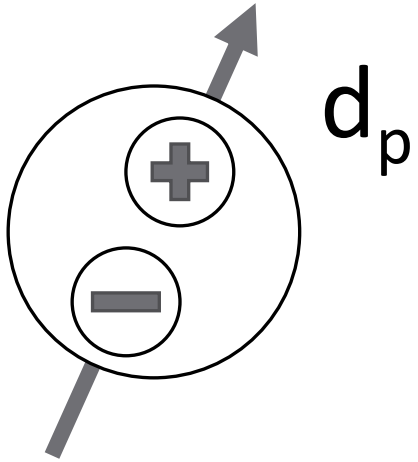

d_p

Sensitivity target

~ 10^{-29} e.cm

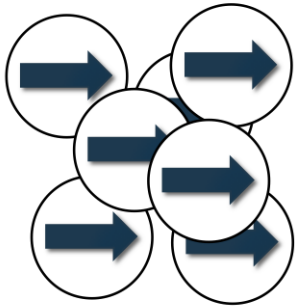

Polarize Beam

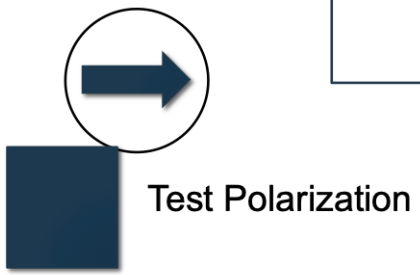

Test Polarization

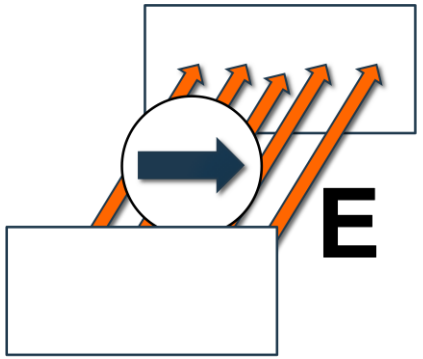

Continuous E field
Interaction over ~ 1000 s

Continuous
Polarization
Measurement

Current Polarimeter

- JePo (JEDI Polarimeter)

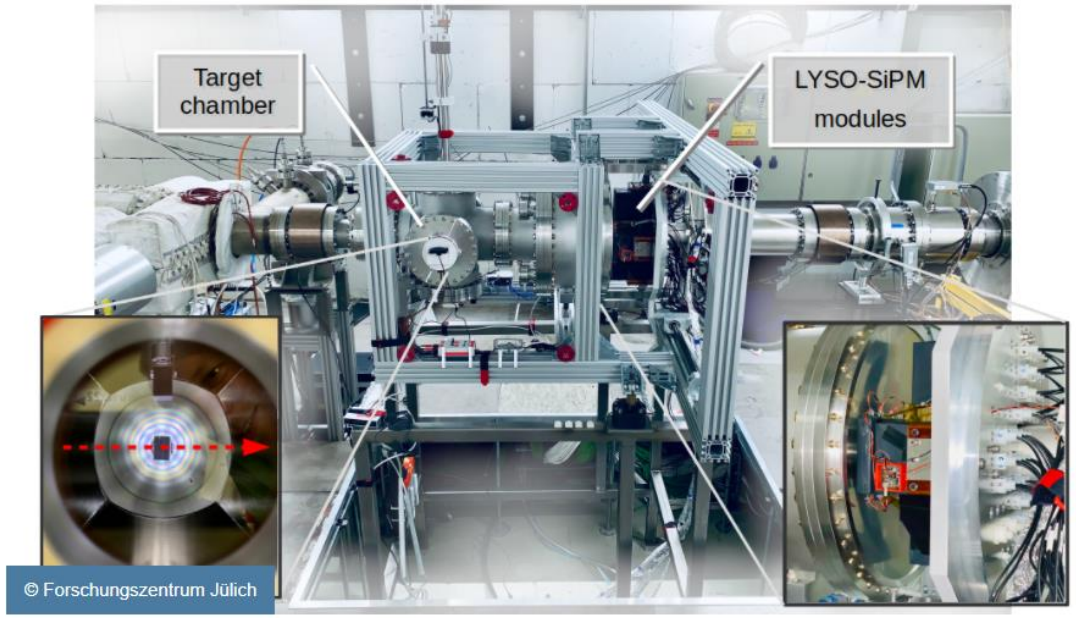

www.jara.org/en/research/fame/news/detail/JEDI-Polarimeter-installed

- Protons are sampled from the beam and scattered from a carbon target
- Elastic scattering direction is affected by beam polarization
- LYSO calorimeters are used to determine elastic hits
- Plastic scintillator grid measures positions and thus asymmetry
- Level of L/R asymmetry observed indicates beam polarization

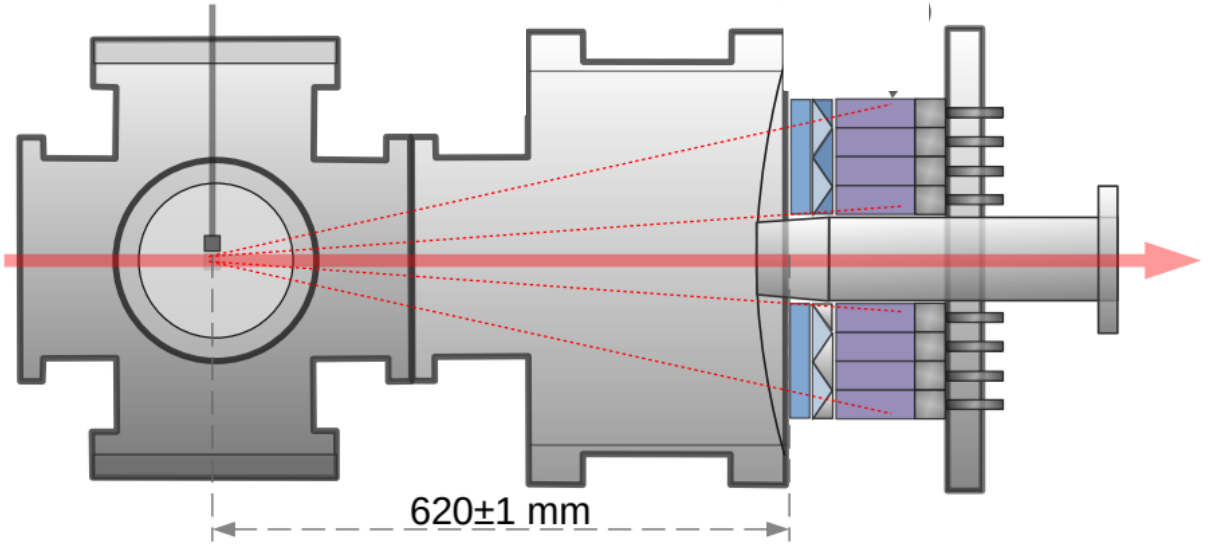

doi.org/10.1088/1748-0221/15/12/p12005

Current Polarimeter

- JePo low energy incompatibility

800µm Steel Beam Window

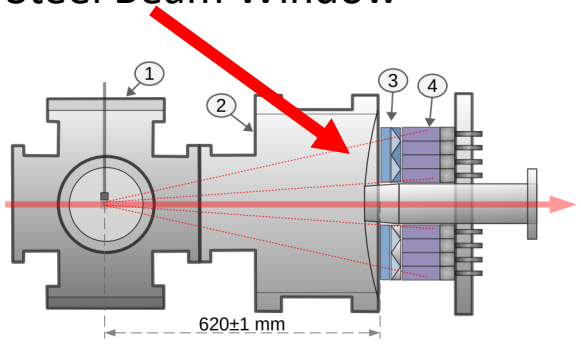

JePo Angular acceptance 4 – 15 degrees

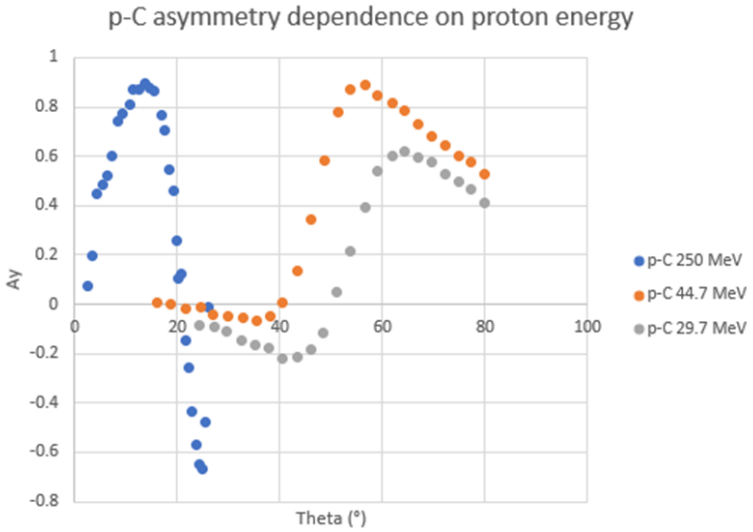

1 Precursor Experiment	2 Prototype Ring	3 All-electric Ring
dEDM proof-of-capability (orbit and polarization control; first dEDM measurement)	**pEDM proof-of-principle** (key technologies, first direct pEDM measurement)	**pEDM precision experiment** (sensitivity goal: 10^{-29} e cm)

270 MeV **30-45 MeV** **270 MeV**

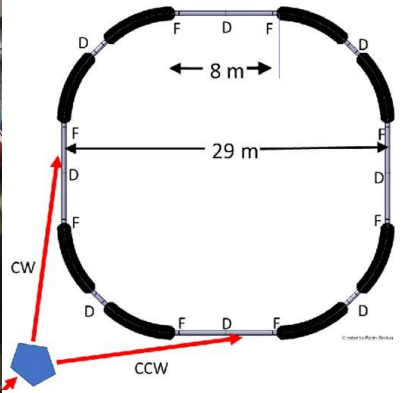

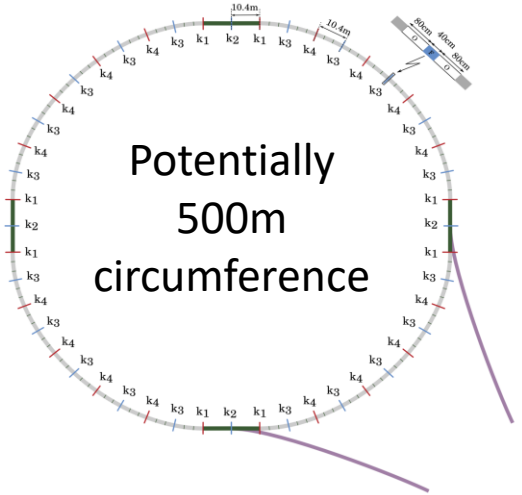

Current Polarimeter

- The necessity of low material budget

- Strong effect from the current 800 um beam window at lower energies
- **Another approach will be needed for low energy**
- In vacuum, low material polarimeter is desirable

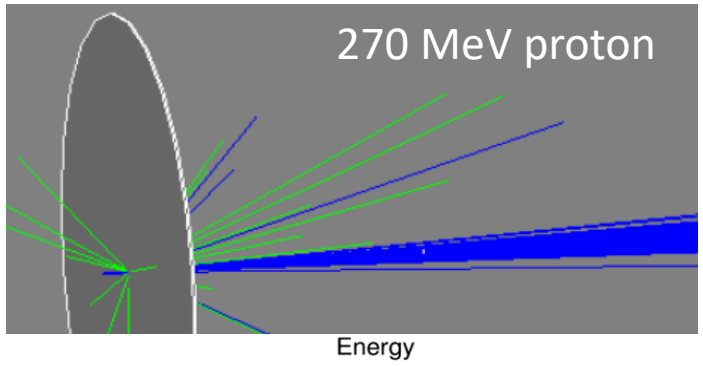

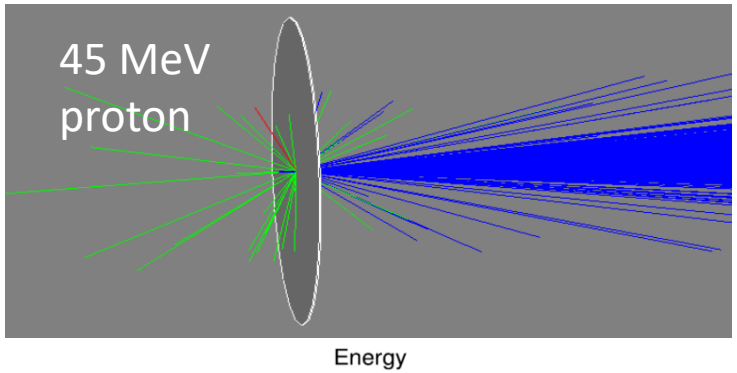

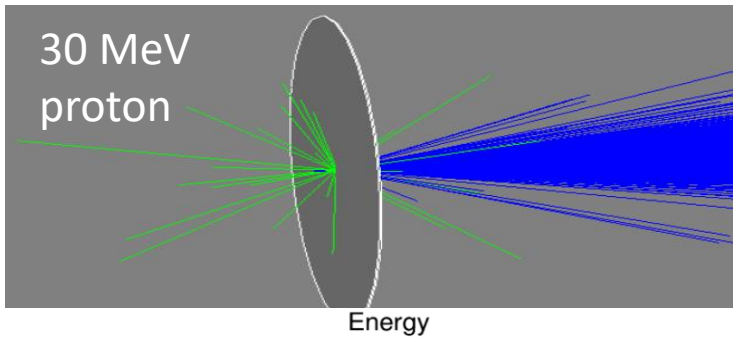

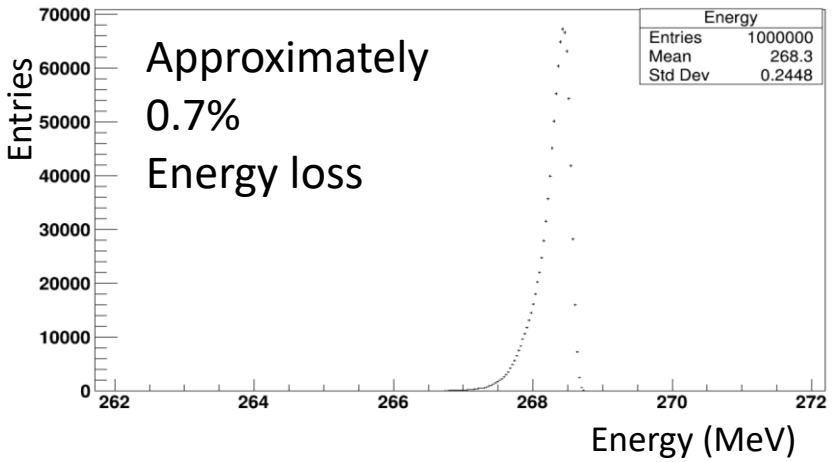

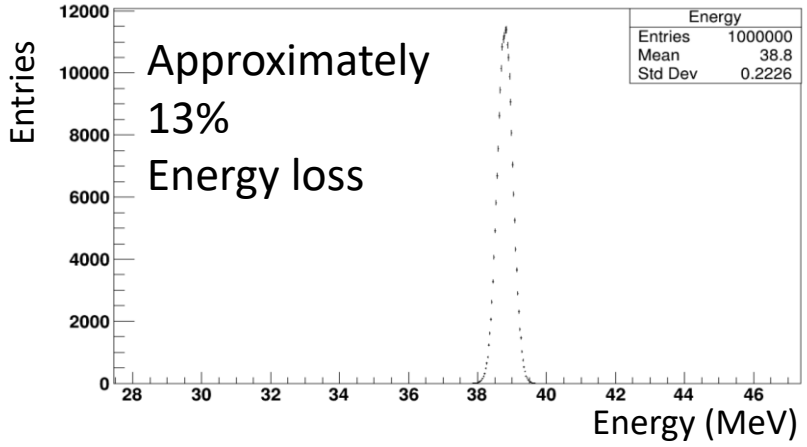

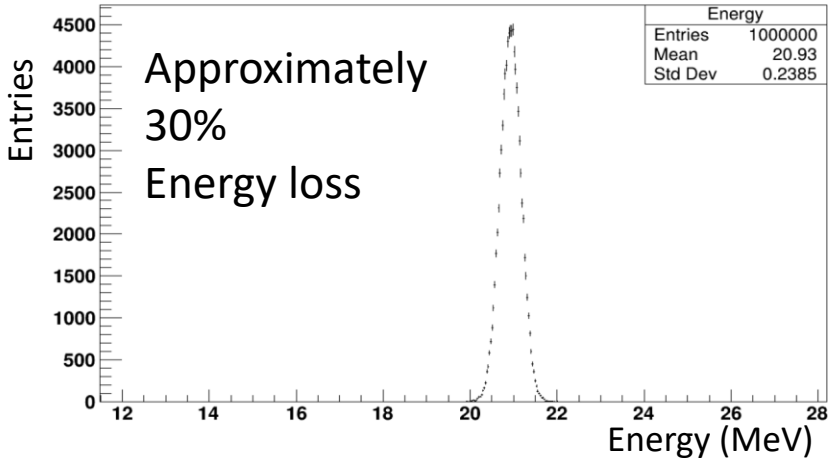

Proposal for a silicon time of flight polarimeter

- Concept and angular acceptance

Not to scale

- HV-CMOS position layer
- LGADs in a time of flight configuration for energy measurement

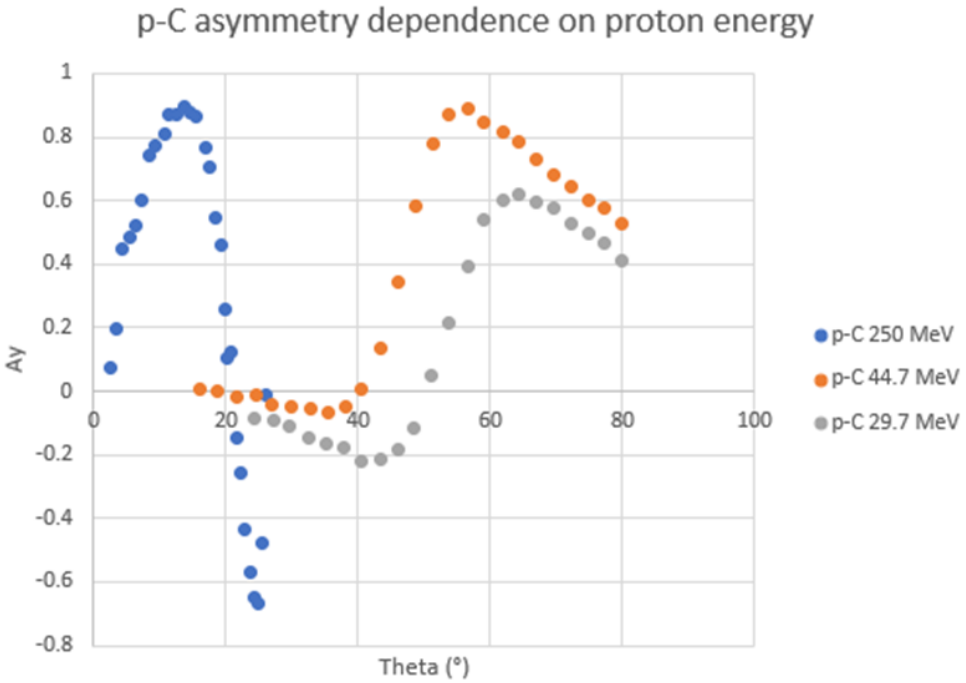

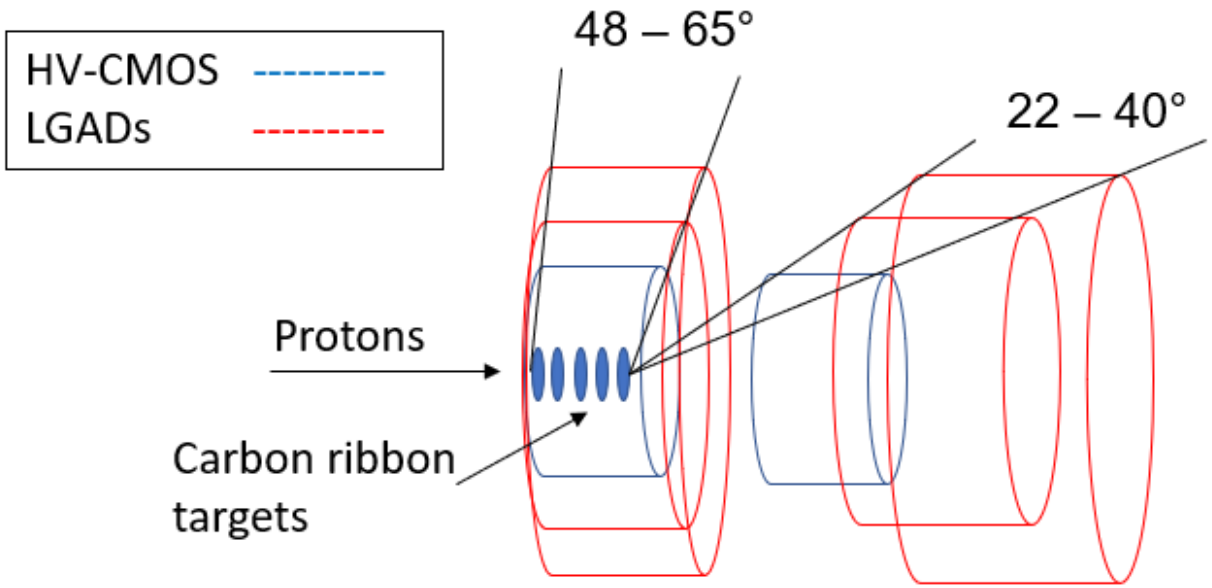

- Ay is the analysing power (the amount of asymmetry that should be observed for a given polarisation at a given angle)
- Thin detectors can be used with minimal angular resolution loss
- 4° – 15° (Current JePo) → ~40 ° – 60° (Low energy polarimeter)
- Surrounding the detector at a lower rate requires larger detection area.

HVCMOS – High Voltage CMOS

- Overview

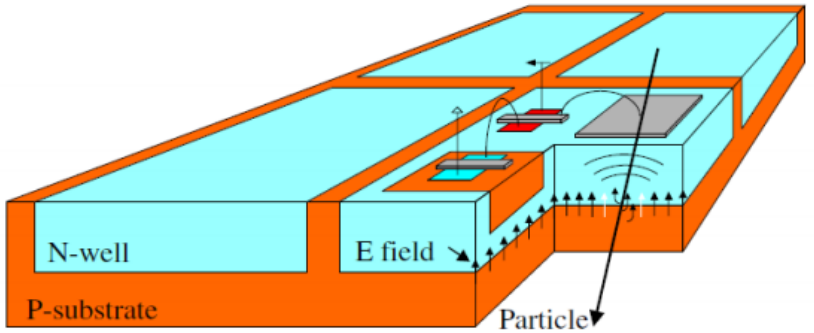

- I. Peric et al (2007)

- CMOS structure inserted in an isolated deep N-Well
- High resistivity wafers in a standard commercial process allow large depletion to be easily achieved at a low cost compared to other detector systems such as hybrid silicon
- Different available options with active development programme in Liverpool

- Small pixel sizes (50µm×50µm)
- Thin modules (>50µm)
- High radiation tolerance (E15 n_eq/cm^2)
- Time resolution (5ns)
- Power consumption (150 mW/cm^2)

LGAD – Low Gain Avalanche Diodes

- Overview

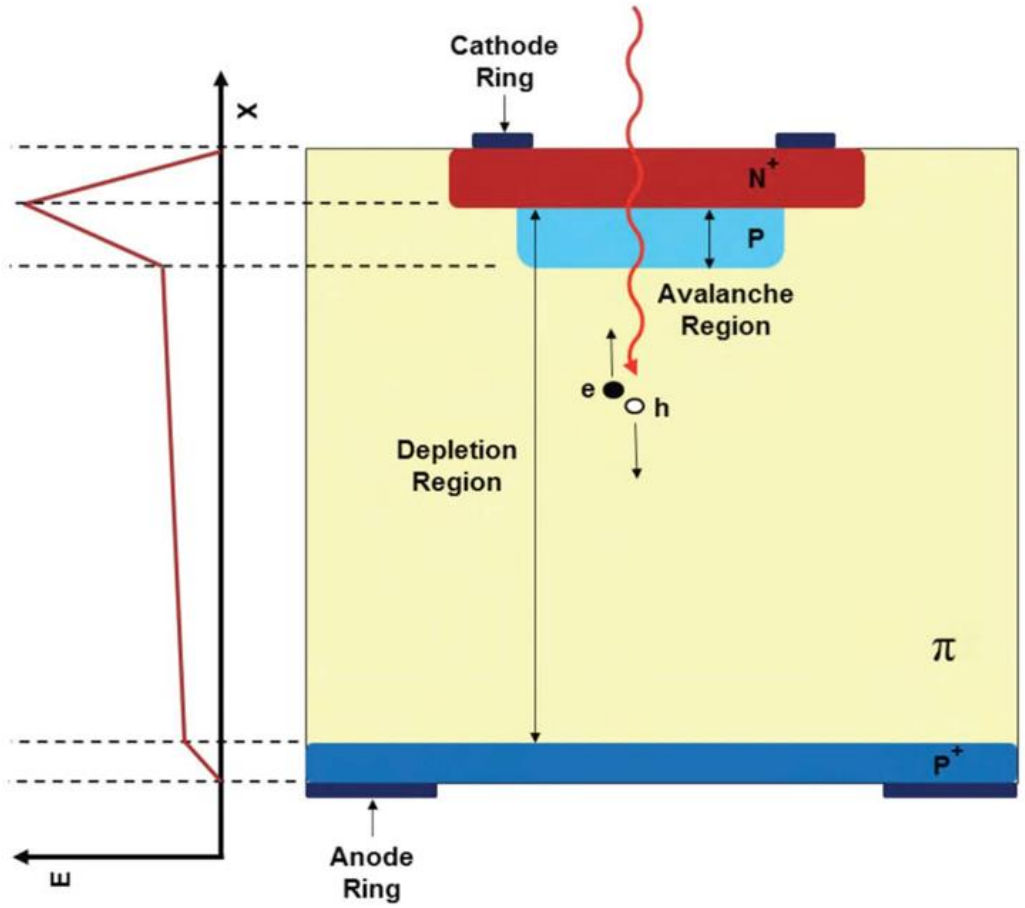

Standard n+ implant is typical for silicon diode detectors.

Heavily doped “P” avalanche/gain region producing typical gains of 10-100.

Excellent time resolution in the order of tens of ps.

Sensors can be thinned < 300 µm

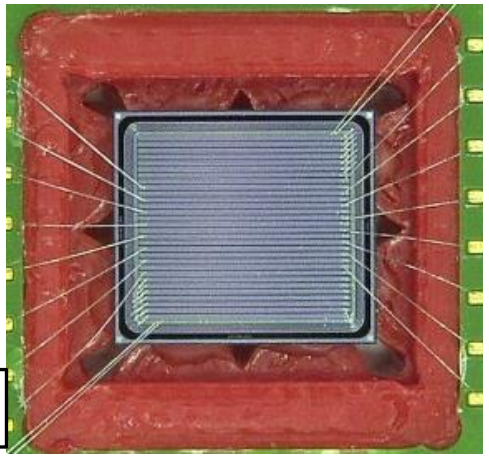

UFSD2 LGAD

http://scipp.ucsc.edu/~schumm/talks/atlas/LGAD/SCHUMM_CPAD-2018.pptx

Low energy polarimeter

- Simulation

- Assumed LGAD time resolution 30-50 ps
- A suitable energy resolution of 3% can distinguish between elastically scattered events that can be used for the
- Determine suitable flight length for polarimeter application

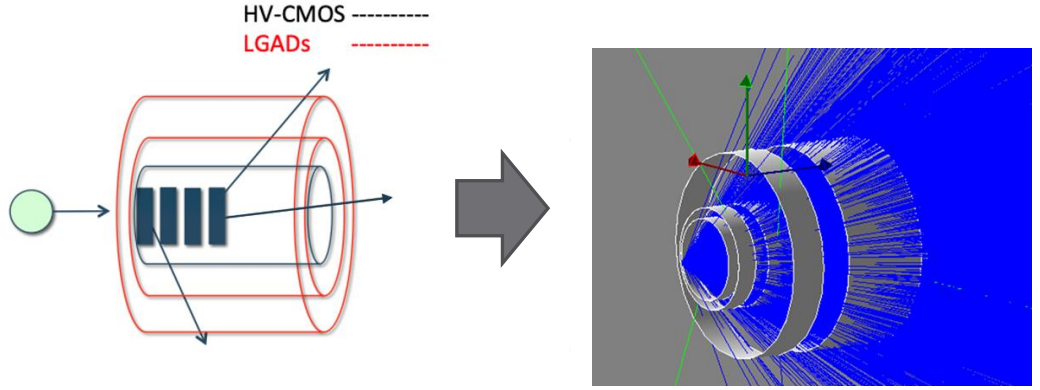

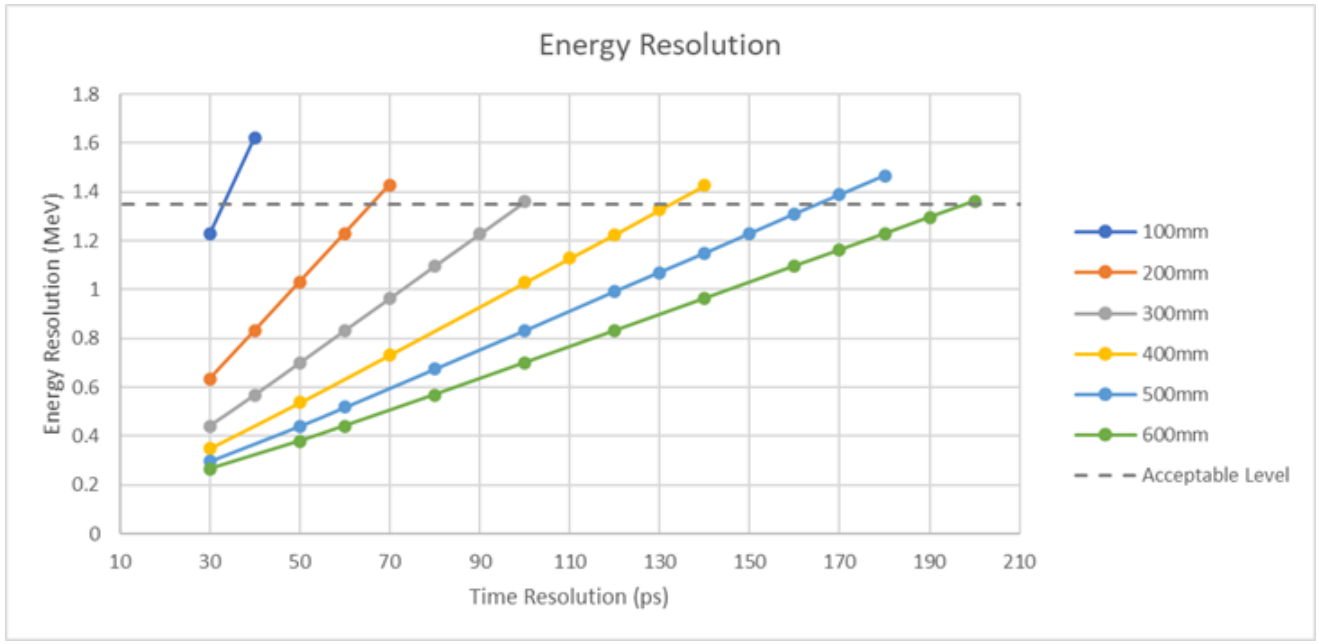

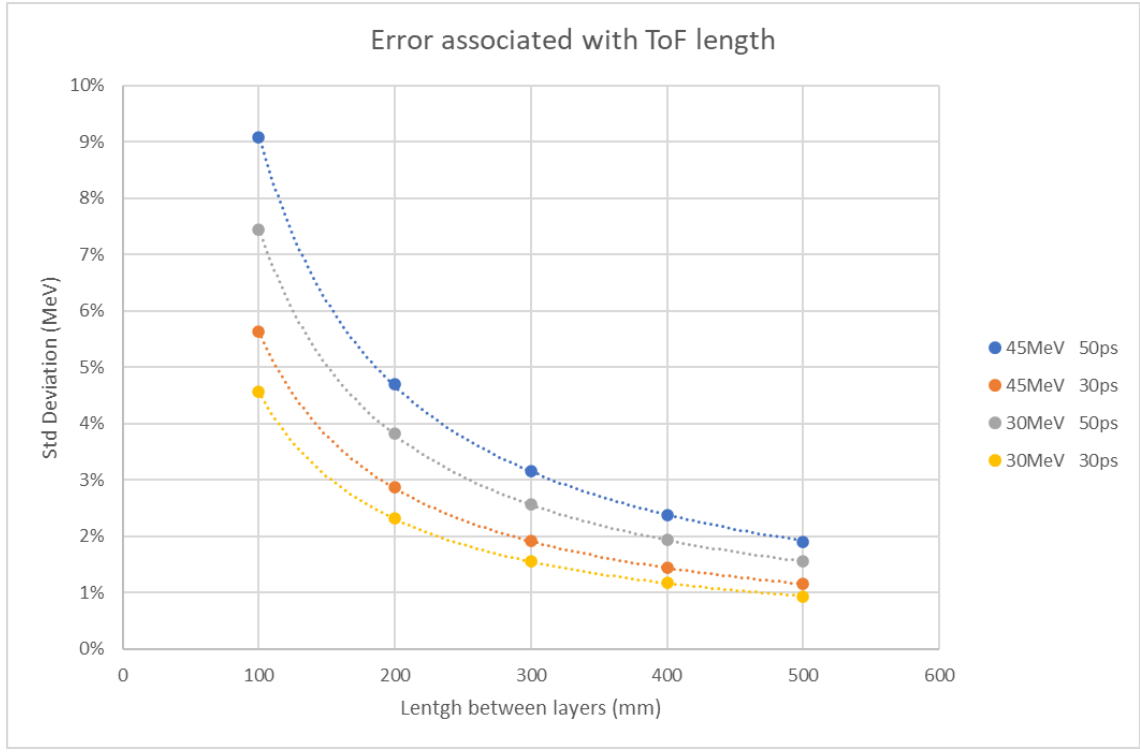

Low energy polarimeter

- Simulated Position Resolution

No strict angular resolution is needed (current detector has 1mm resolution)

Position layers help with tracking for energy measurement and give excellent angular resolution regardless

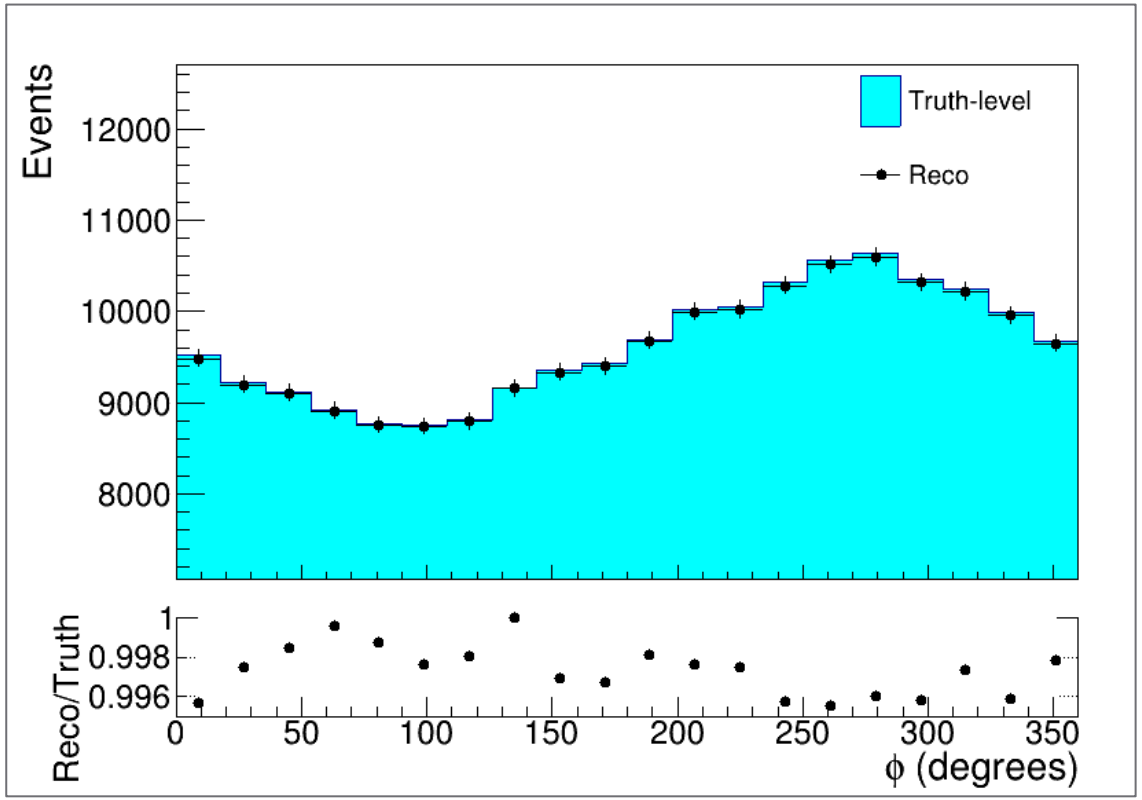

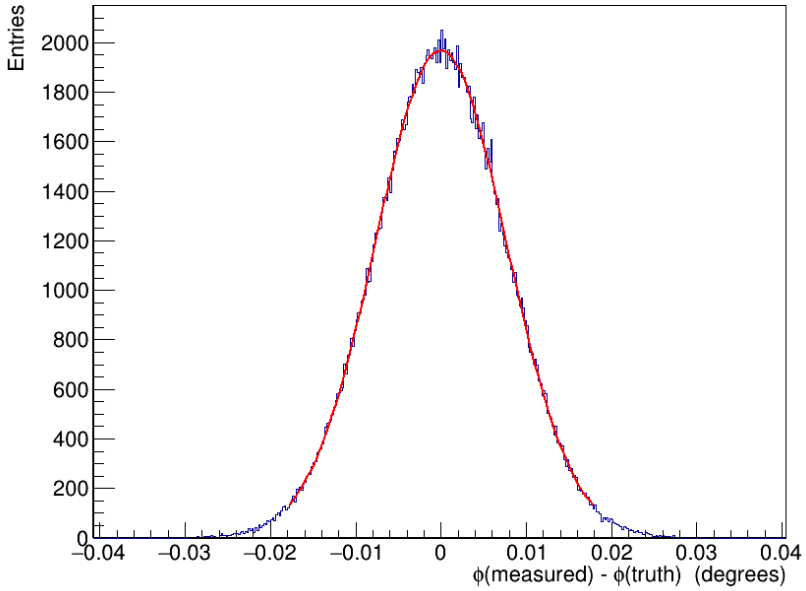

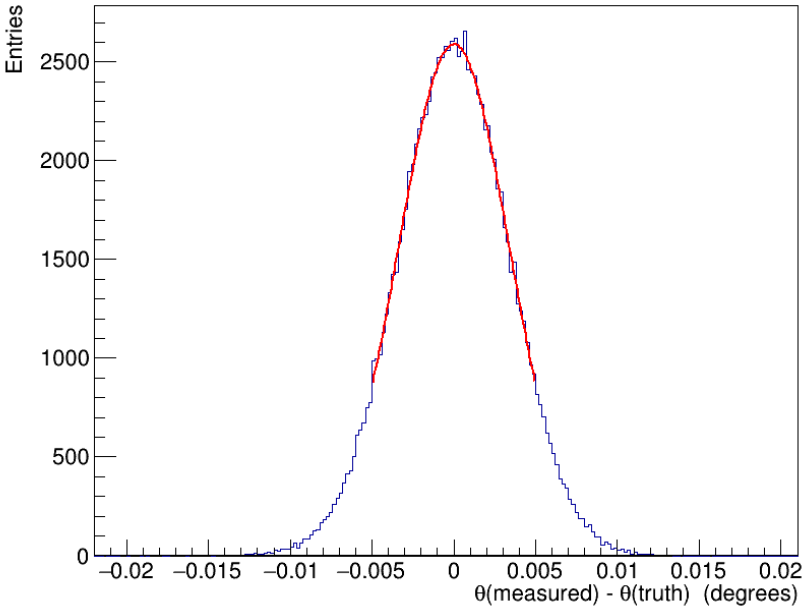

LGAD Time of Flight telescope

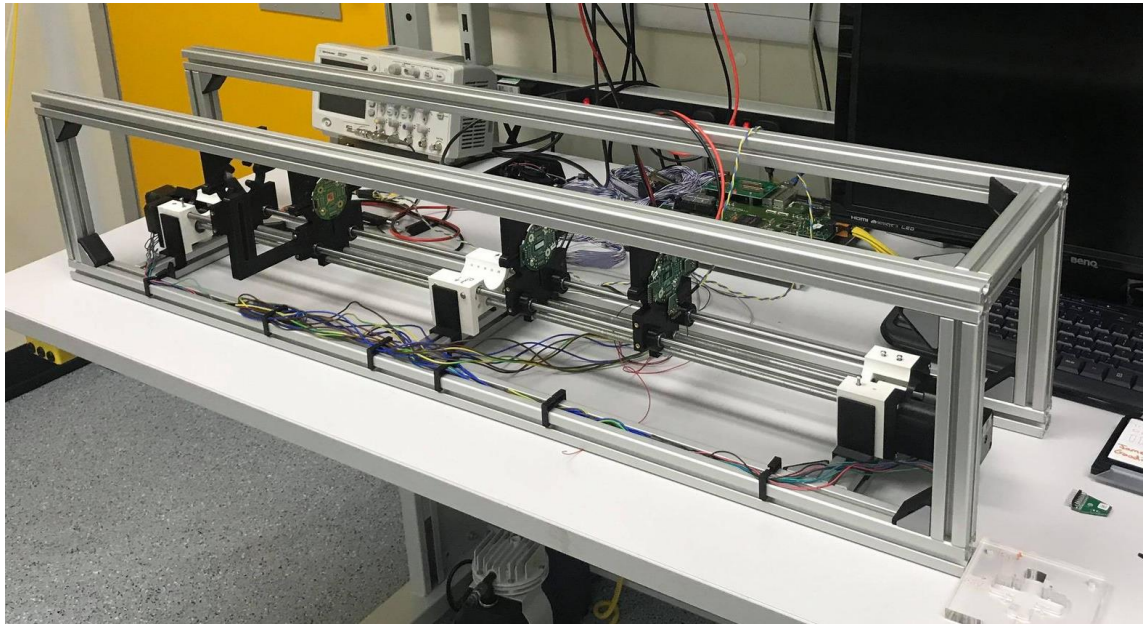

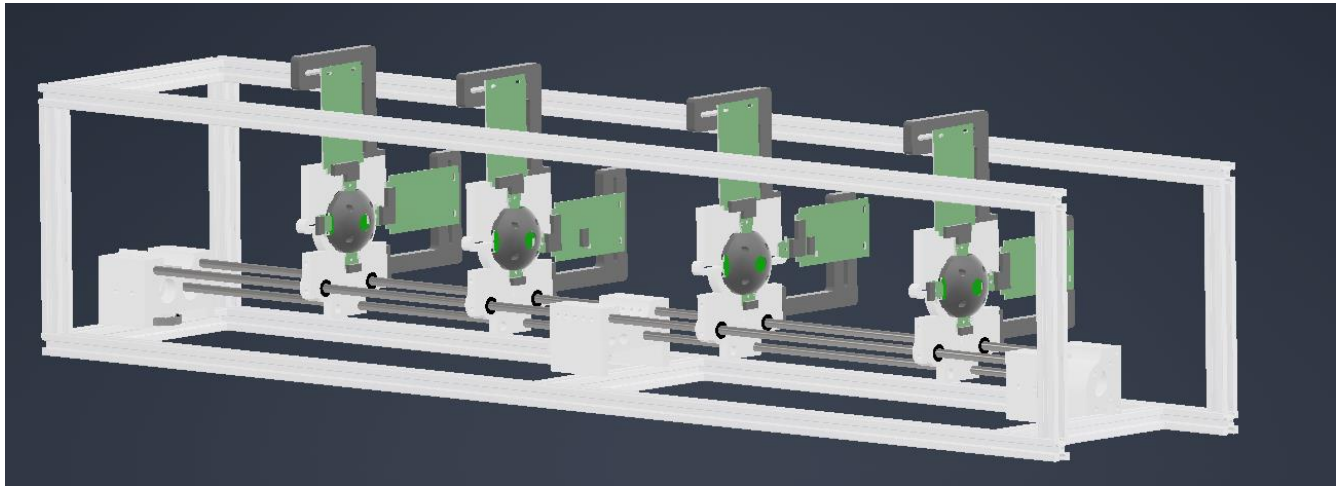

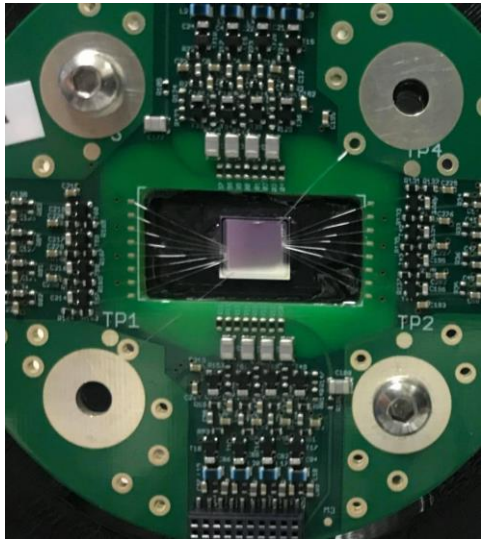

LGAD sensors are USFD2 provided by FBK

Two variations:

- 30 strip, 146 um pitch, 5 mm length
- 20 strip, 216 um pitch, 15 mm length

LGAD Time of Flight telescope

- Readout

Extra information:
http://jspc29.x-matter.uni-frankfurt.de/trb/publications/201310_NoMeTDC_Ugur.pdf

TRB3 TDC module

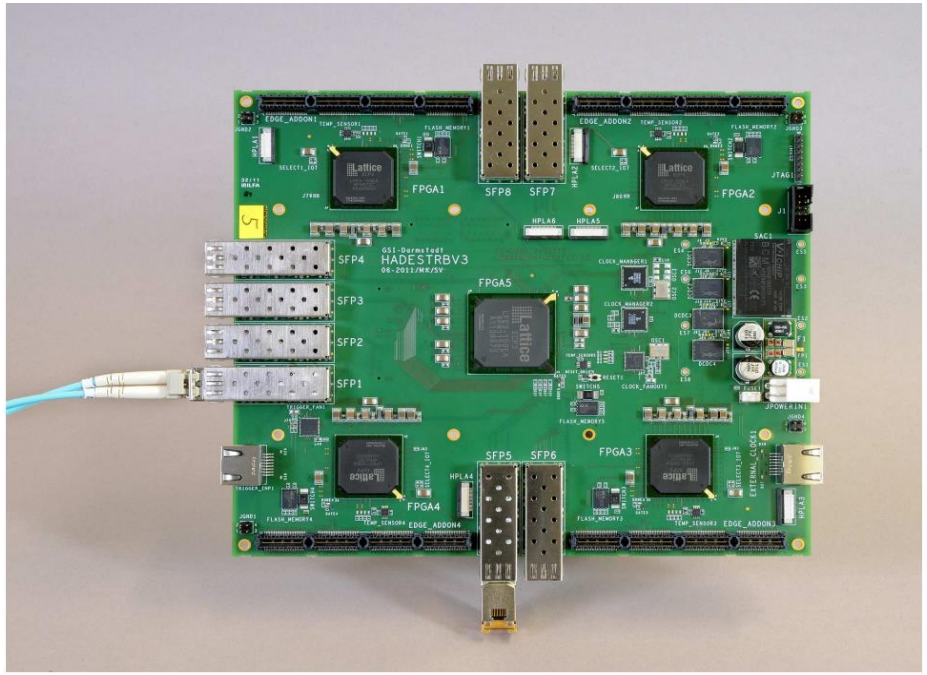

M Traxler et al 2011 JINST 6 C12004

The third addition to Padiwa-family boards, optimized for direct connection to a MC-PMT - four of these 16 channel boards fit onto the 5x5 cm2 backside of a typical MC-PMT

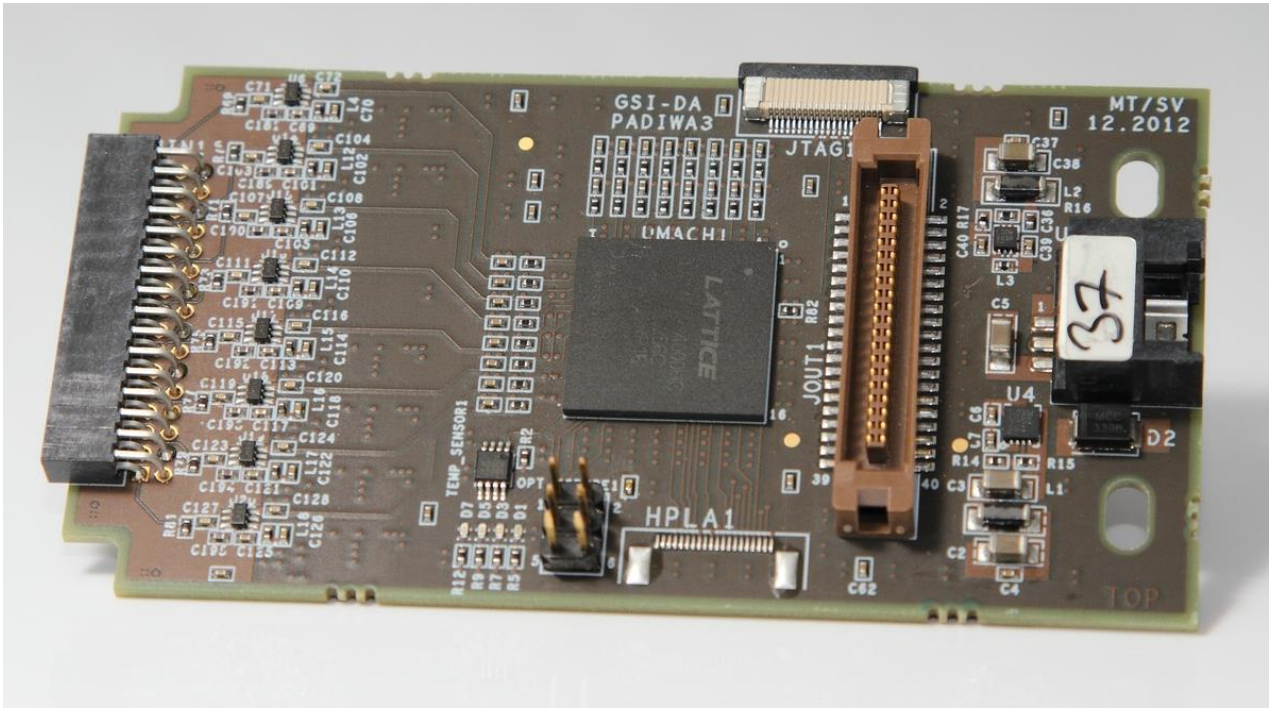

LGAD Time of Flight telescope

- Sr90 testing

- Initial testing with a strontium-90 beta source
- Good signals pre-amplified on sensor carrier PCB
- Signals have a good enough SNR for input into PADIWA readout

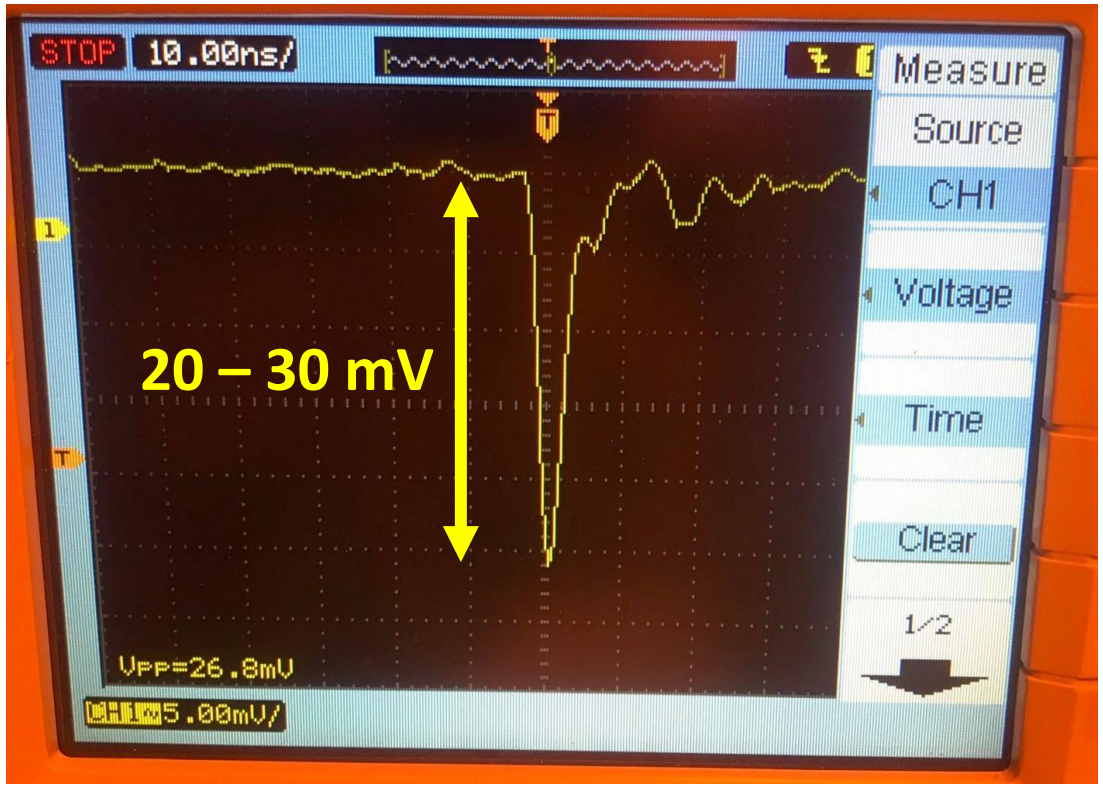

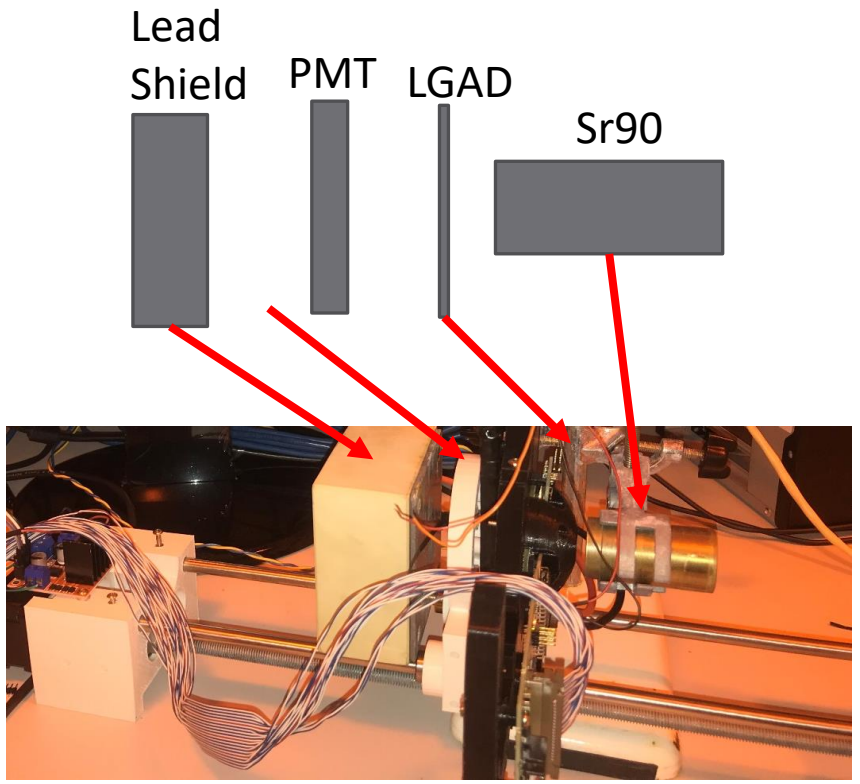

LGAD Time of Flight telescope

- Sr90 testing

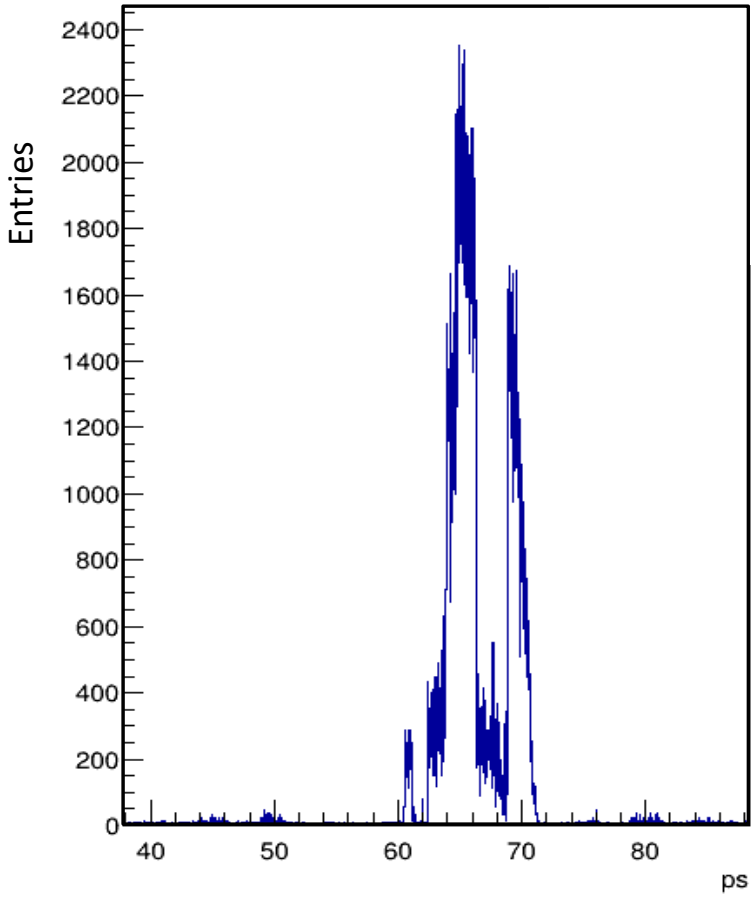

Coincidence results of Sr90 between two layers positioned only 10mm apart.

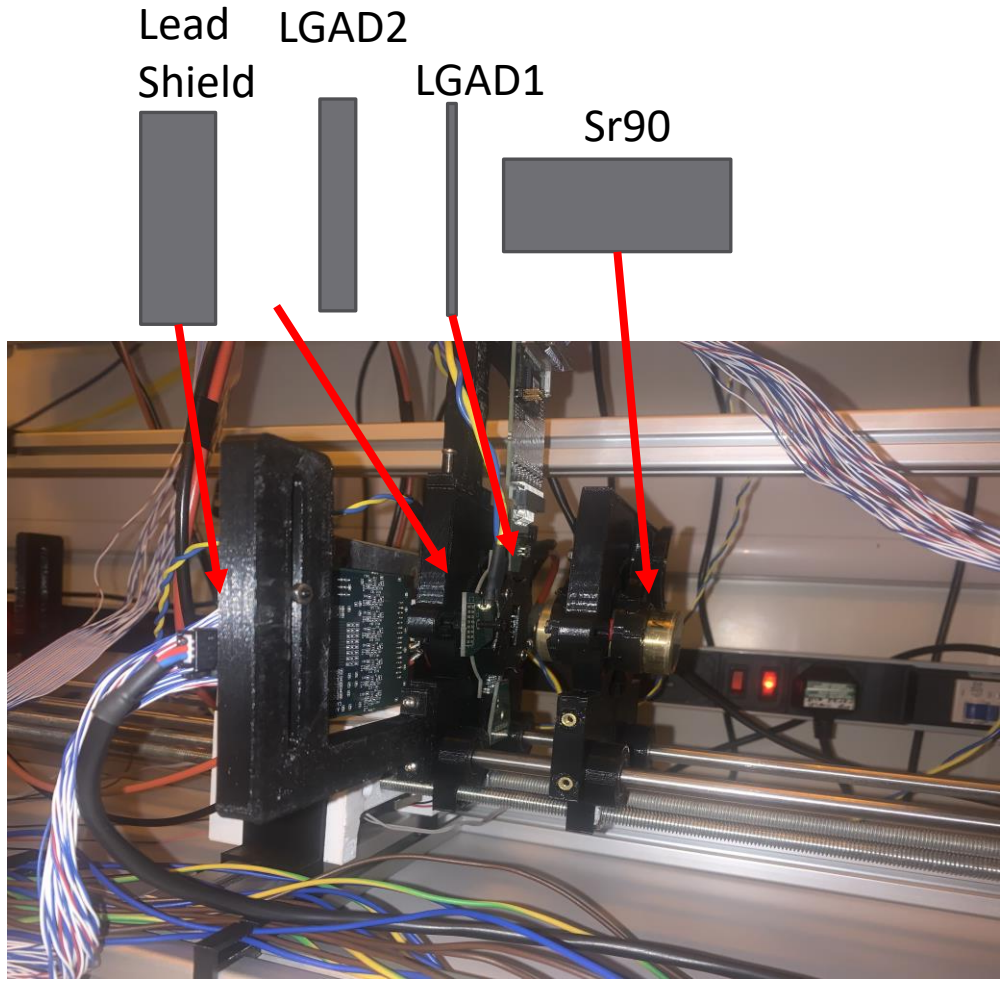

LGAD Time of Flight telescope

- Testbeam and particle ID

- Using spare (out of hours) proton beam time at Rutherford PLC Cancer Treatment centre in Northumberland
- First testbeam measurements with the LGAD ToF telescope was conducted
- Results currently being analysed
- Poor placement for direct proton measurement
- Telescope observed particles with different time over threshold times possibility that our detectors observed many types of particles and particle identification could be preformed

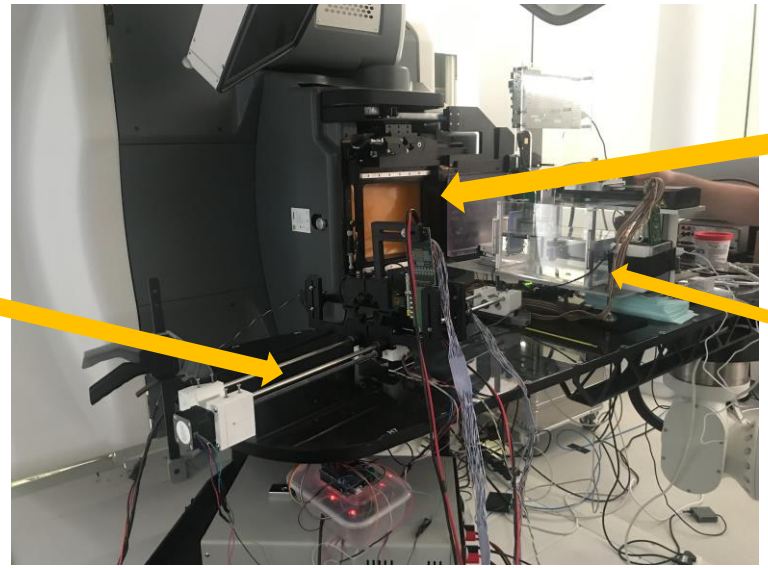

Thank you for listening!
Any Questions?

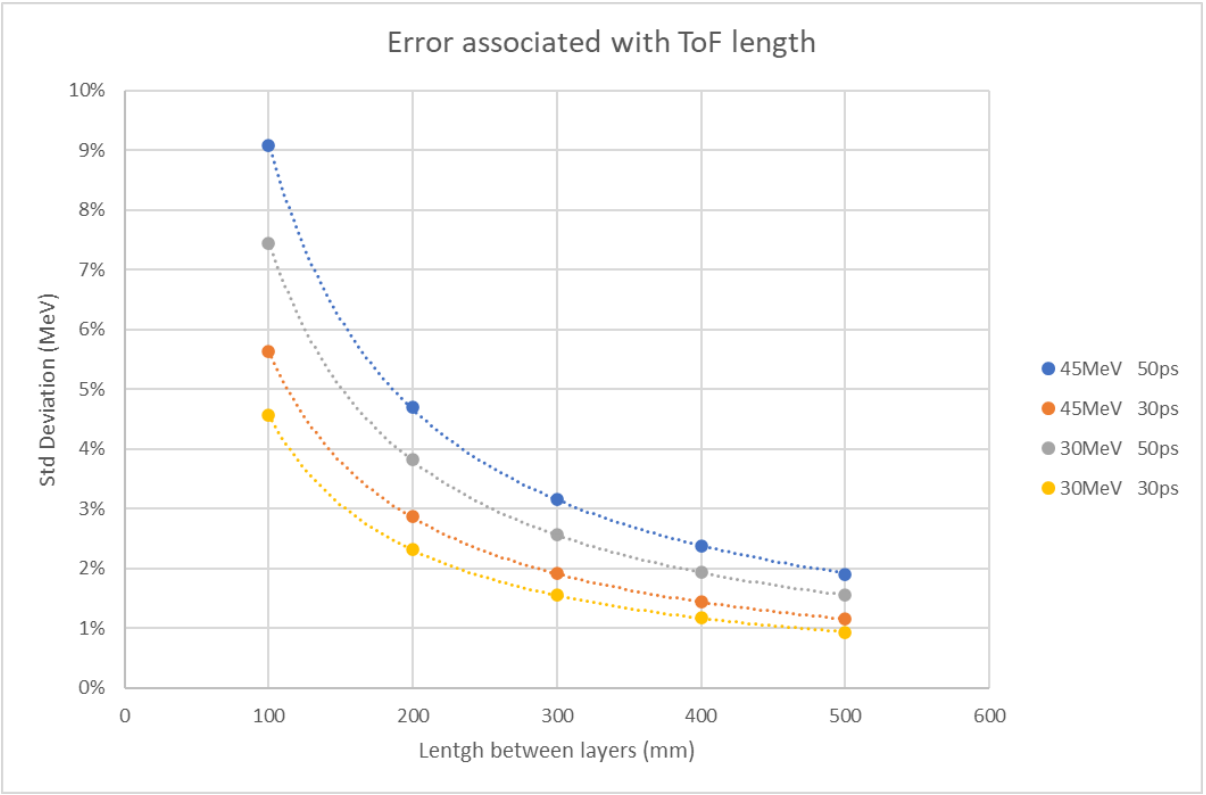

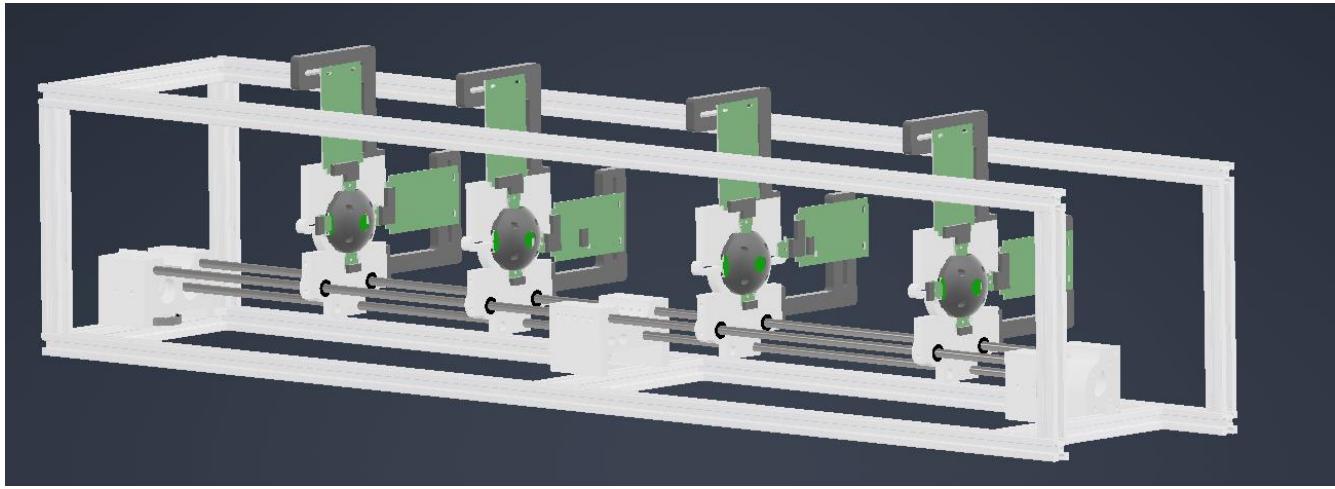

Backup Slides

Telescope LED/Laser Calibration

Green LED flashes:

- 10 mV signal height
- Rising edge measured can be set to omit oscillation and calibrate time differences between detectors

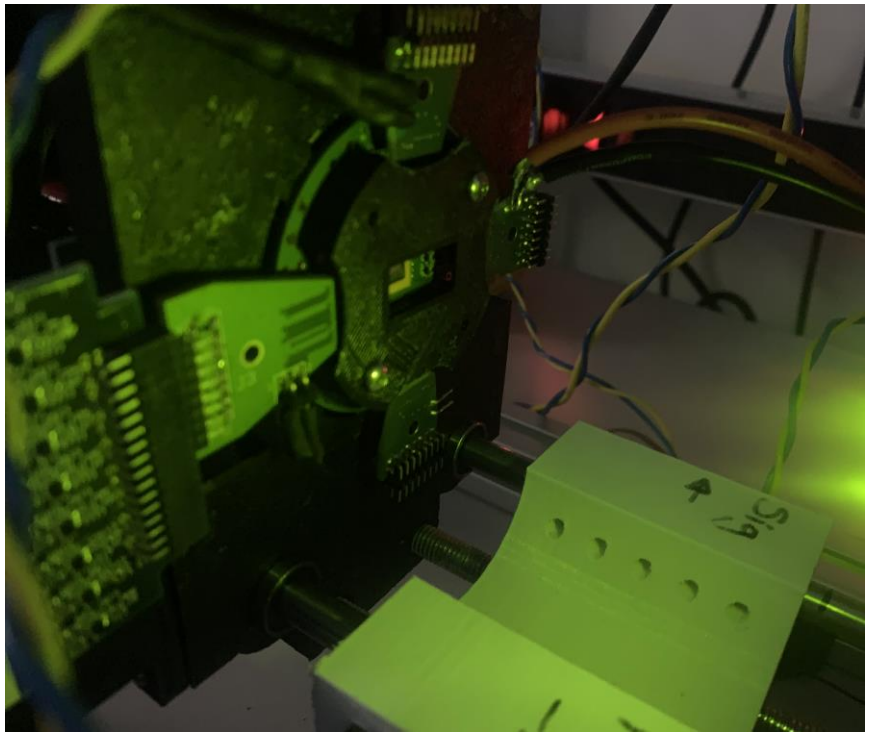

LGAD Time of Flight telescope

- Split target simulations

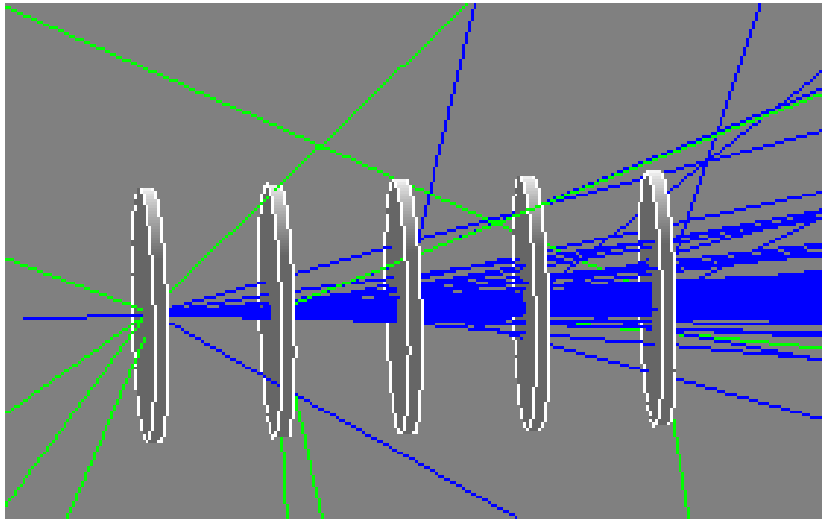

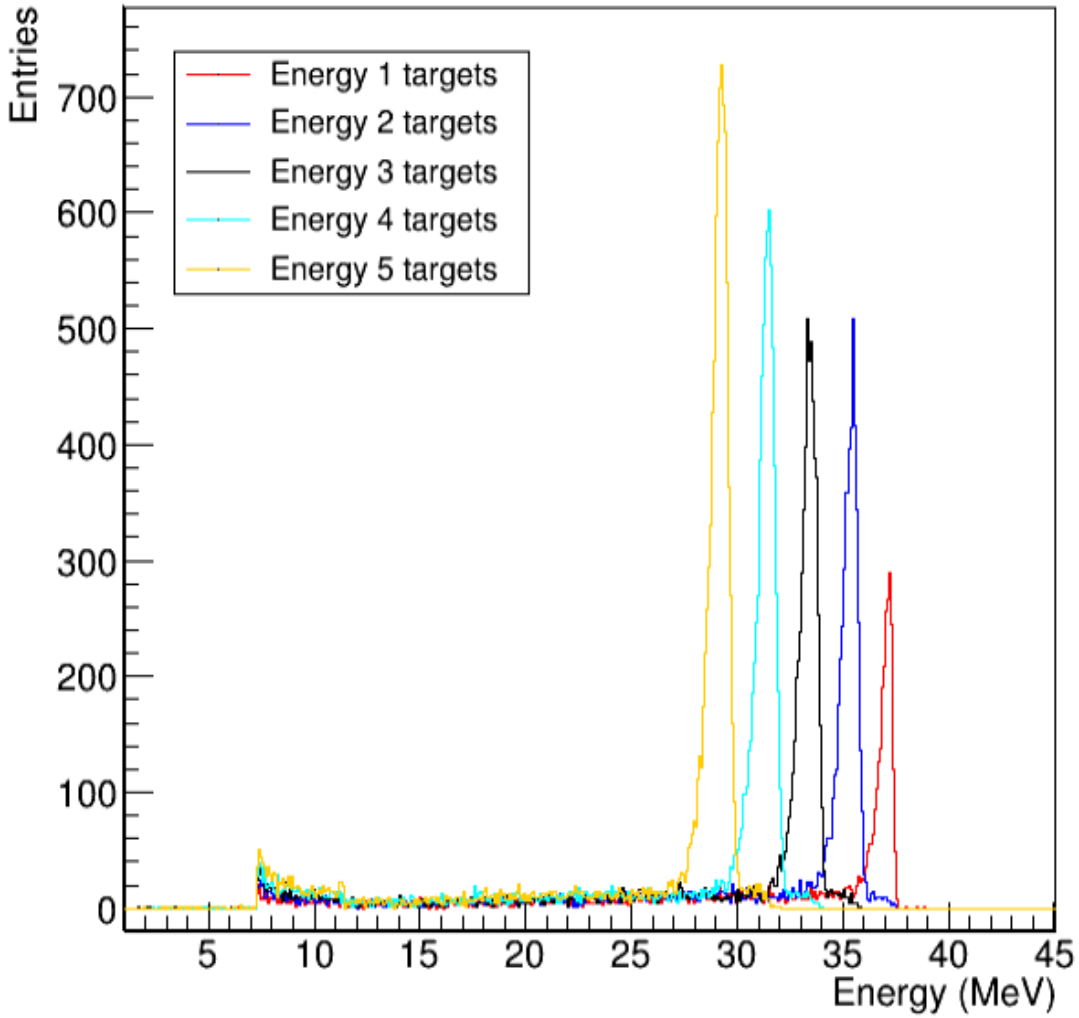

LGAD Time of Flight telescope

- Simulated time resolution

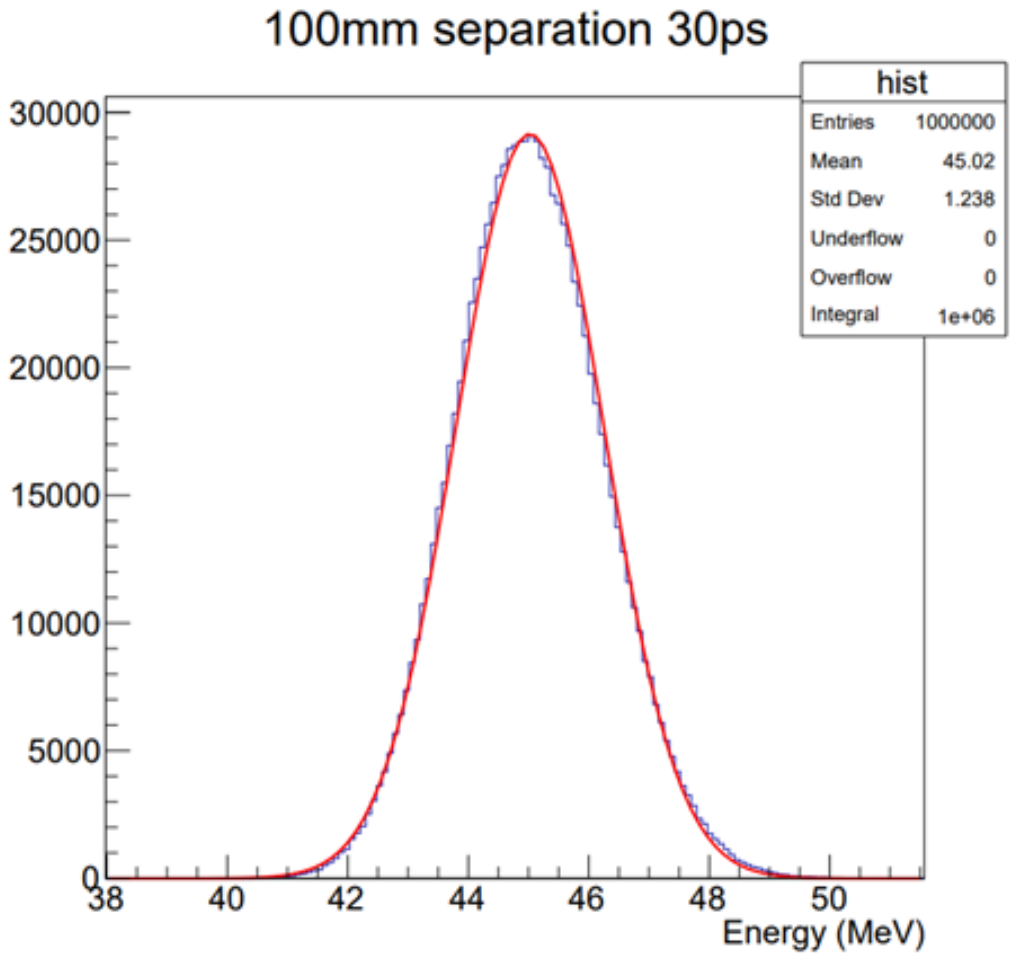

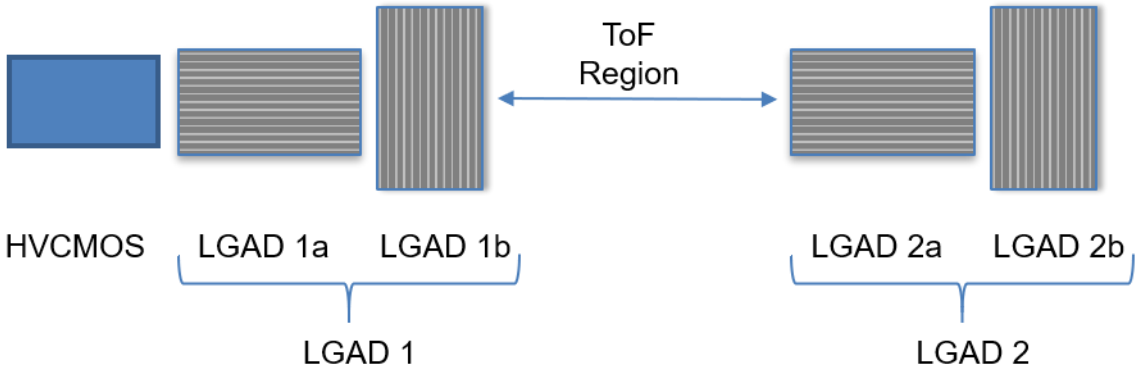
ToF
Region
HVCMOS
LGAD 1a
LGAD 1b
LGAD 2a
LGAD 2b
LGAD 1
LGAD 2

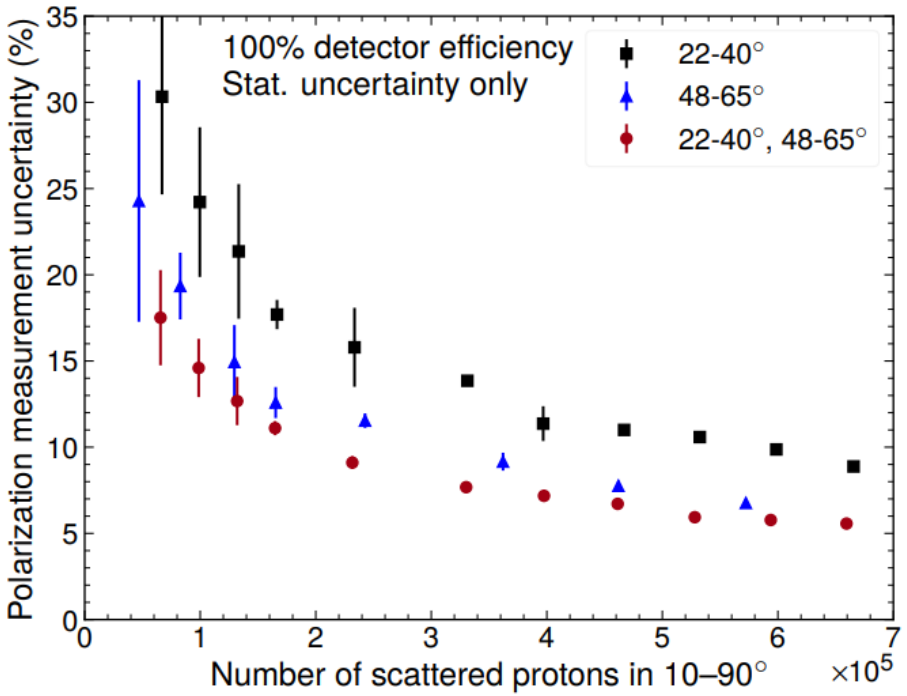
100% detector efficiency
Stat. uncertainty only
22-40°
48-65°
22-40°, 48-65°
Polarization measurement uncertainty (%)
Number of scattered protons in 10–90°
×10^5
0
5
10
15
20
25
30
35
0
1
2
3
4
5
6
7

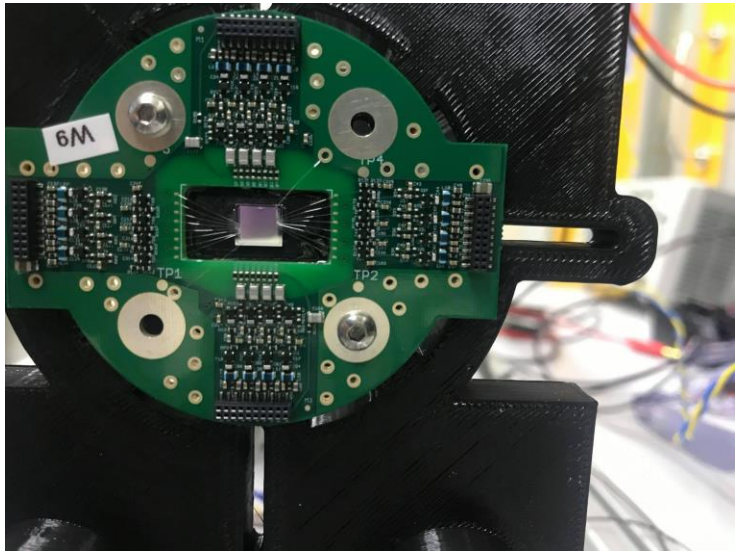
W9
TP1
TP2

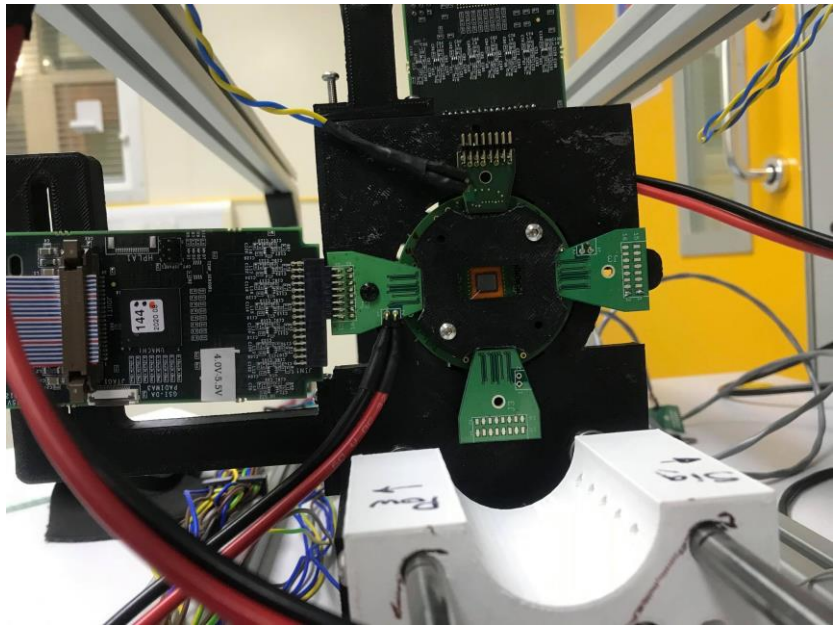

Telescope control GUI

Si3Po

Easy and precise carriage movement to position sensors

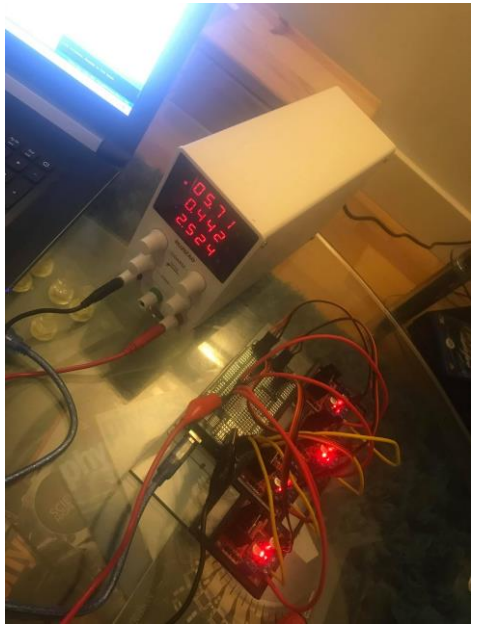

Movement 0

- CAR 1 LEFT
- CAR 1 RIGHT
- CAR 2 LEFT
- CAR 2 RIGHT
- CAR 3 LEFT
- CAR 3 RIGHT
- CAR 4 LEFT
- CAR 4 RIGHT

ToF Controller

Carridge 1 z 0

Carridge 2 z 0

Carridge 3 z 0

Carridge 4 z 0

- HOME

LED Flash Delay 0

LED Flasher

Laser Flash Delay 0

Laser Flasher

ManualControl

Var1 0

Var2 0

Var3 0

Var4 0

- COMMAND1
- COMMAND2
- COMMAND3
- COMMAND4
- COMMAND5

Carridge [Carridge]

Car1Pos 0

Car2Pos 0

Car3Pos 0

Car4Pos 0

- CHECKSTATUS

Secondary beam polarimeter via pellet target

– Influence on primary beam

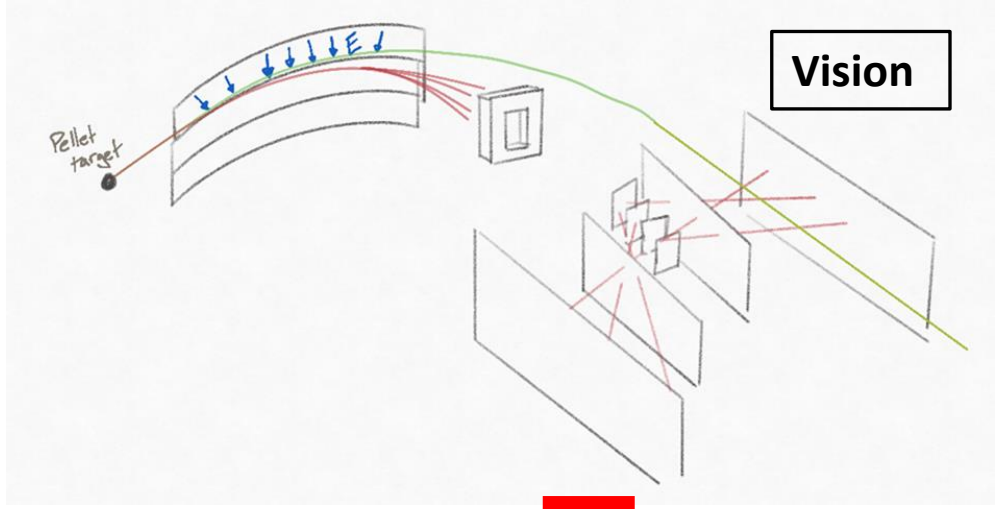

Sampled particles fall slightly out of orbit

Tiny carbon pellet 20 µm

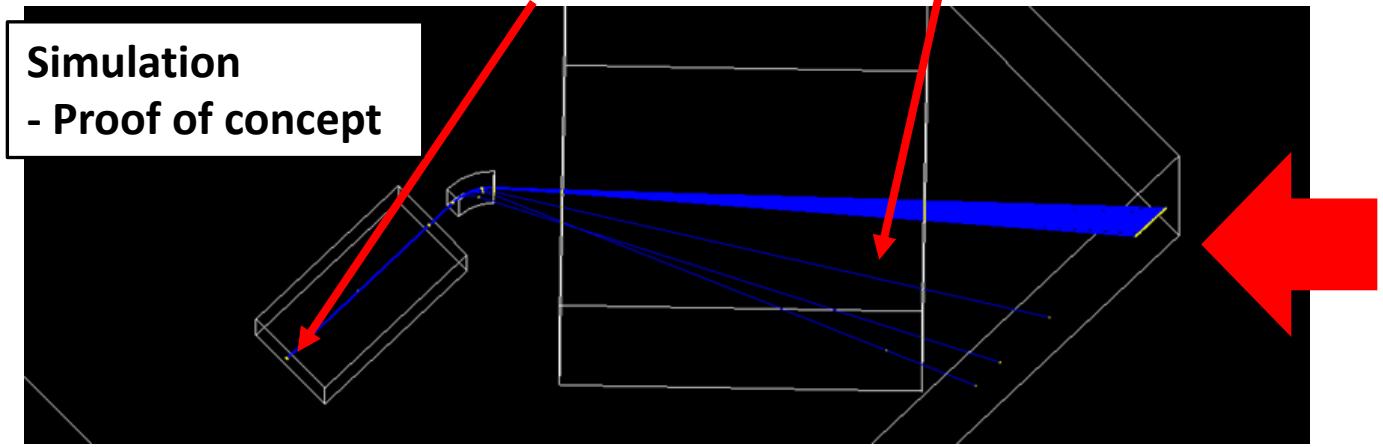

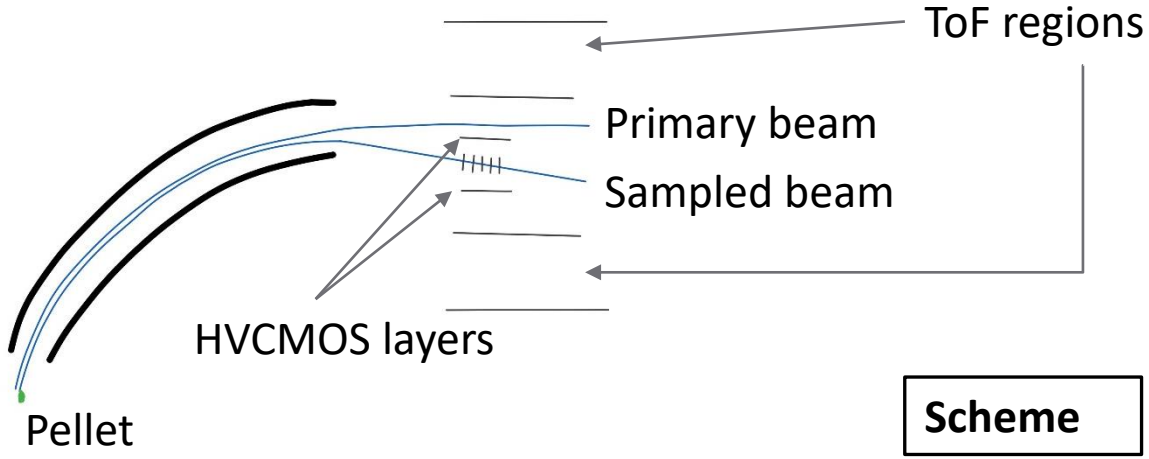

Pellet target feasibility study

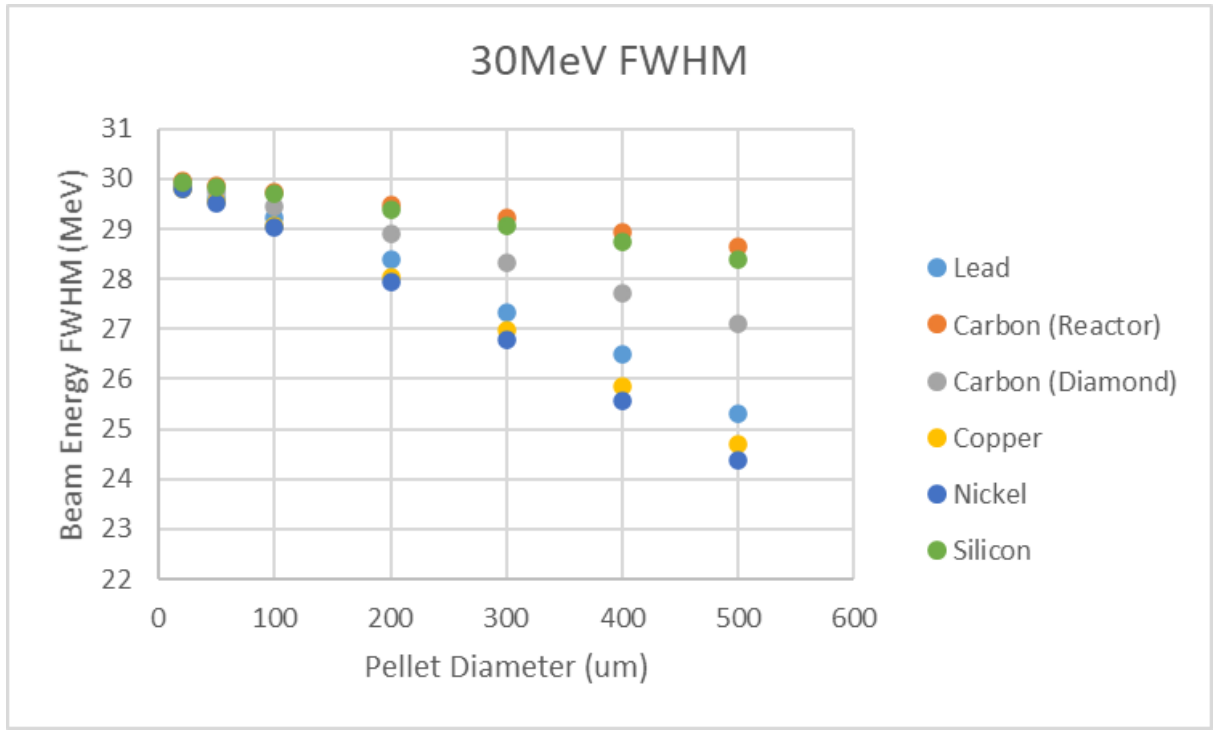

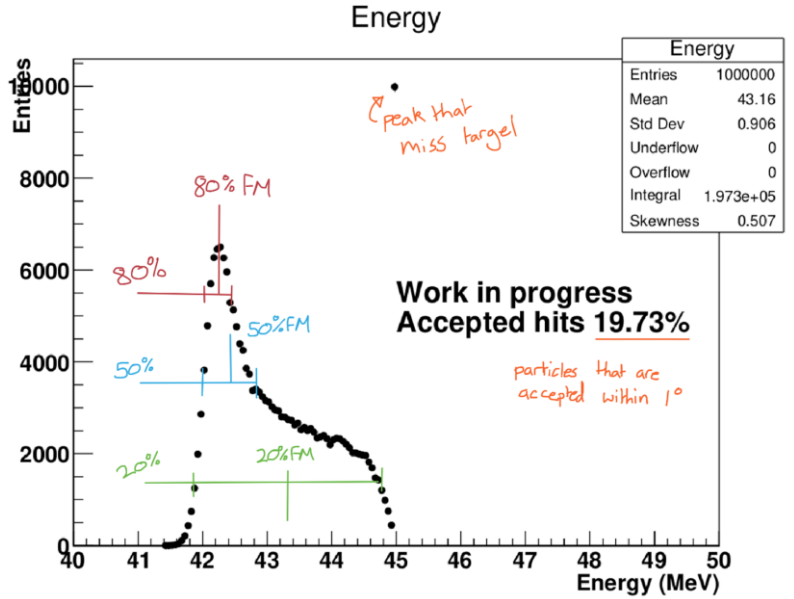

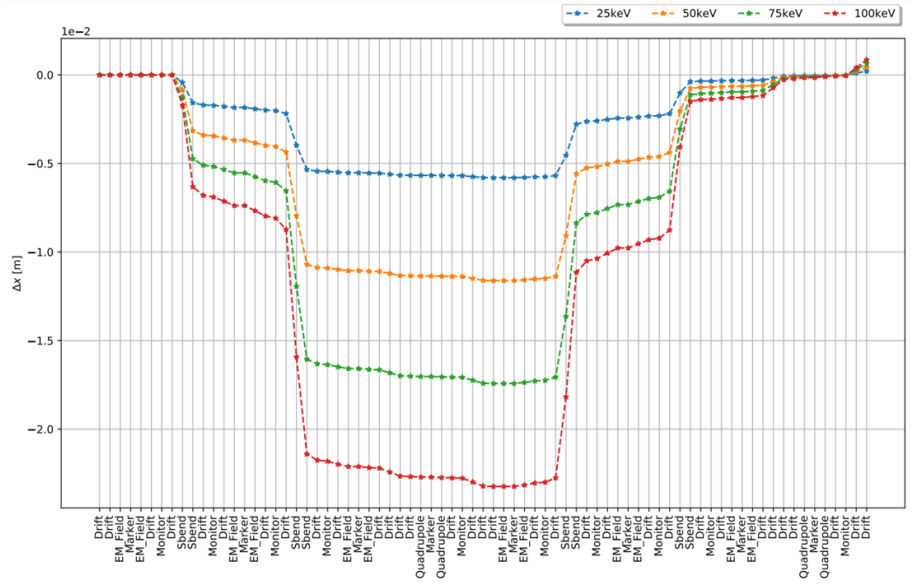

Result:

- Pellet target can achieve 2cm offset from main beam whilst retaining stable circulation (100 keV loss in target)

Simulations by Maximilian Vitz

Configuration

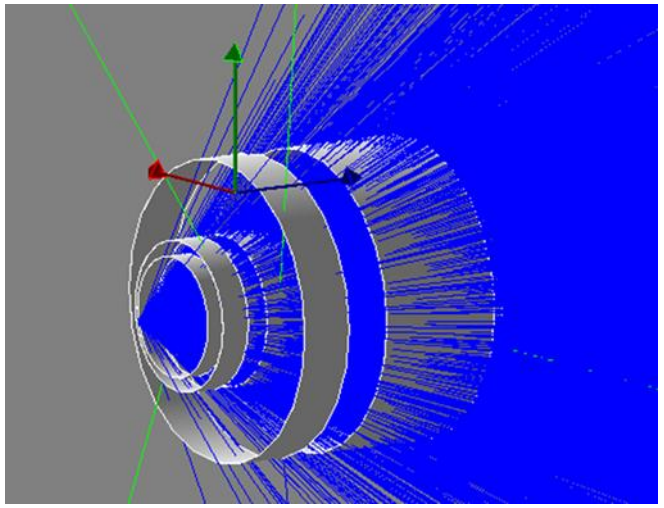

A forward configuration will target only one area of figure of merit

- A cylindrical design surrounding the beamline and target will be effective in two areas of high figure of merit.

- Forward area figure of merit strongly influenced by rate, not analyzing power.

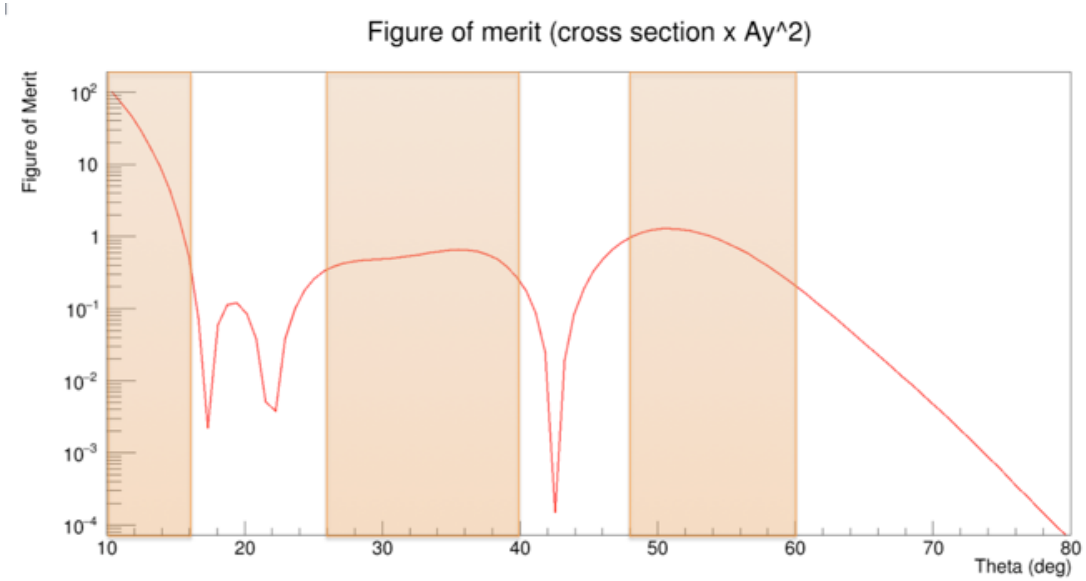

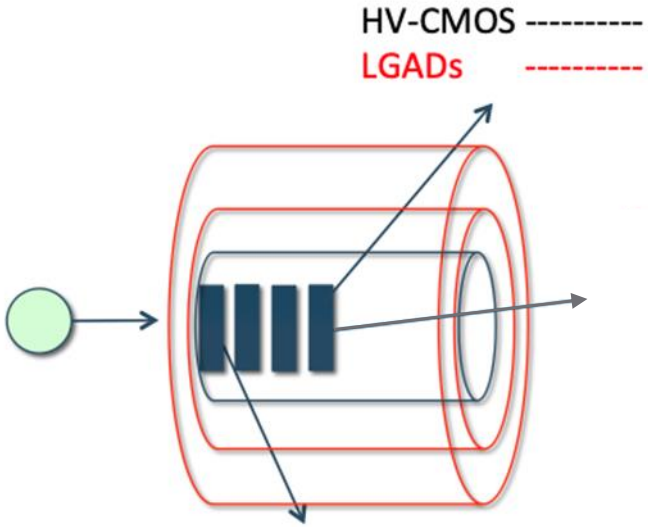

Phi measurement accuracy and efficiency

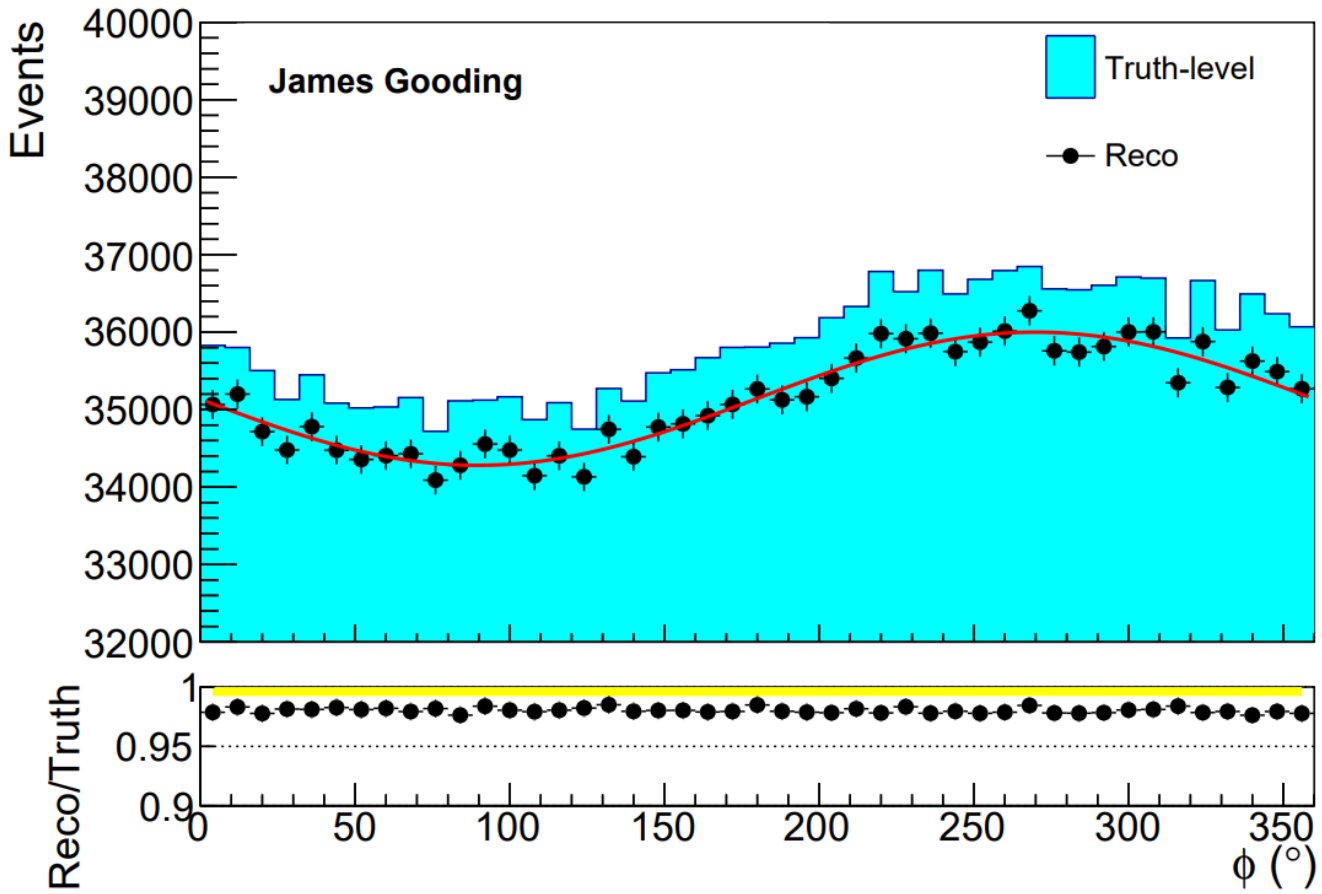

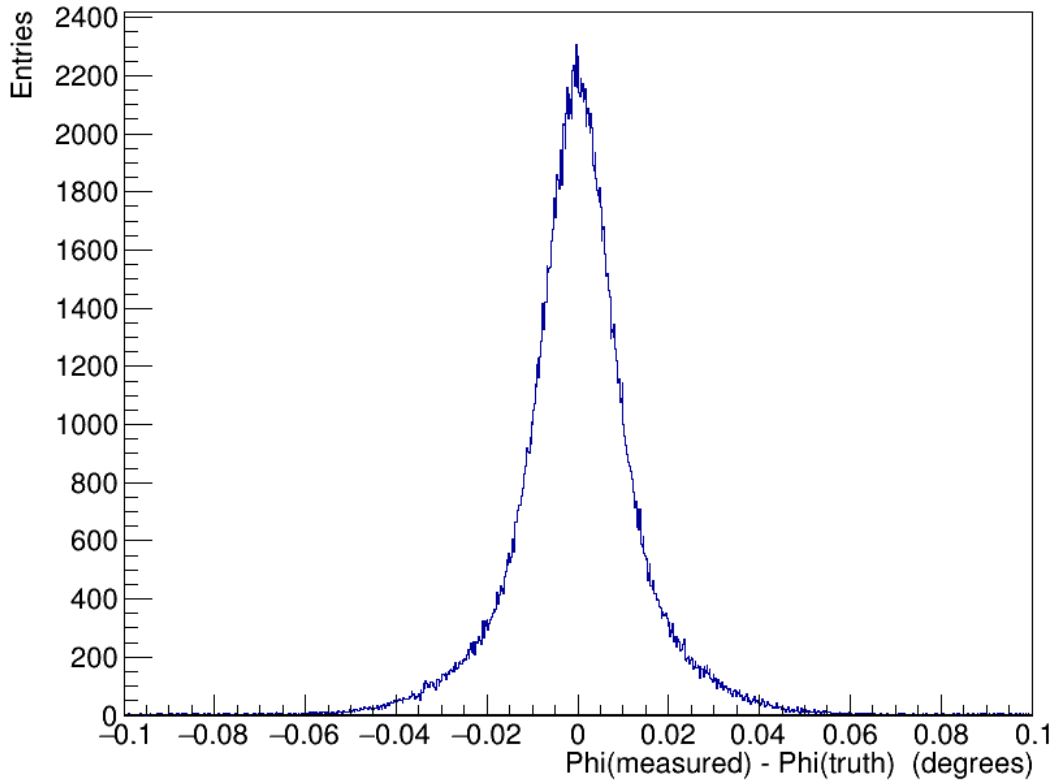

Theta accuracy and efficiency

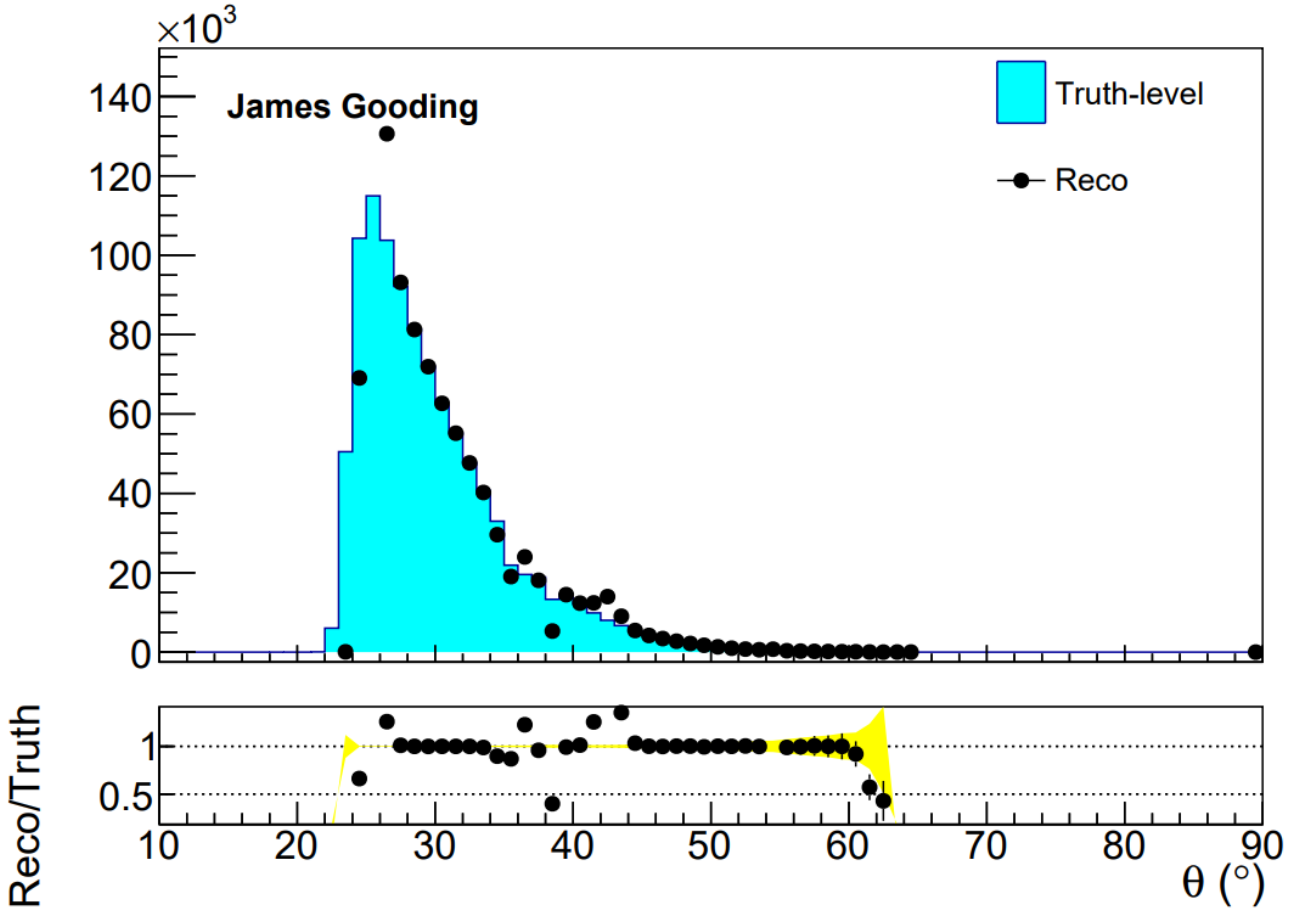

Some theta sections struggle to be reconstructed in sections where there is spacing between cylinders.

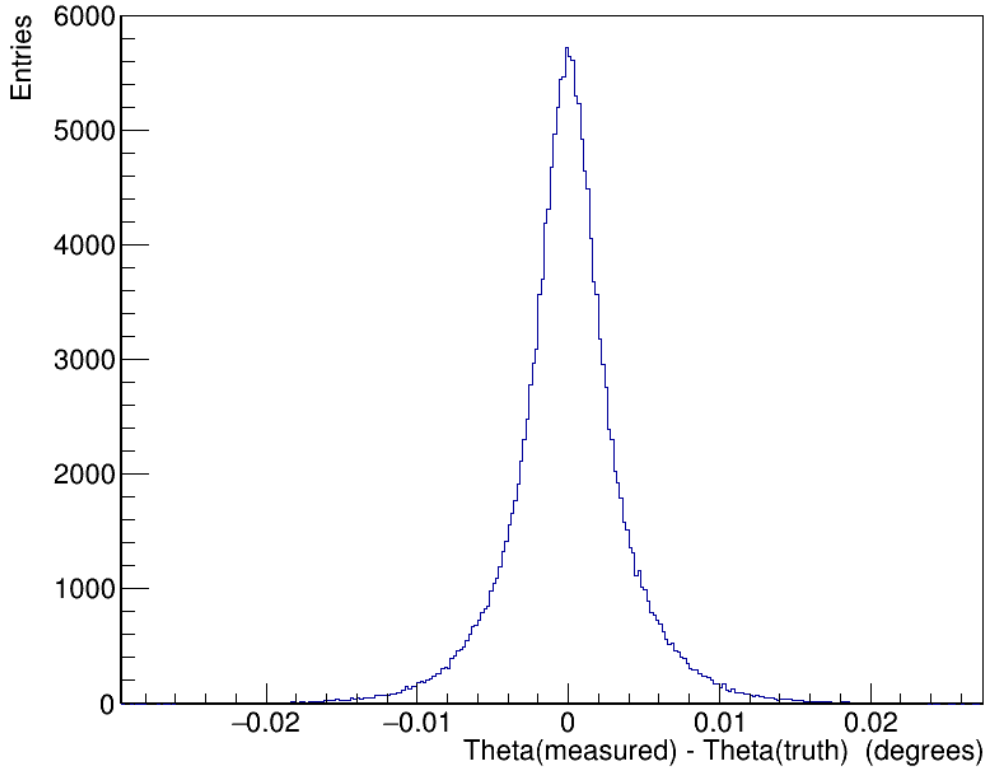

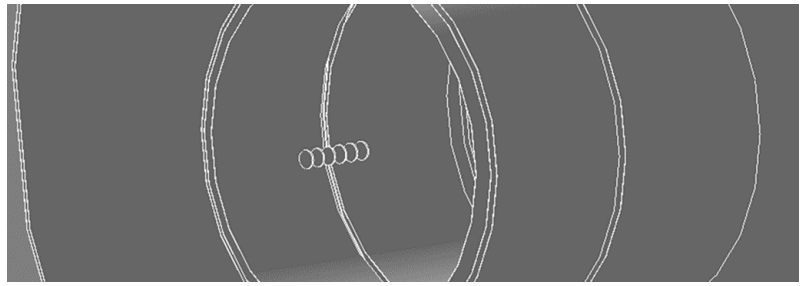

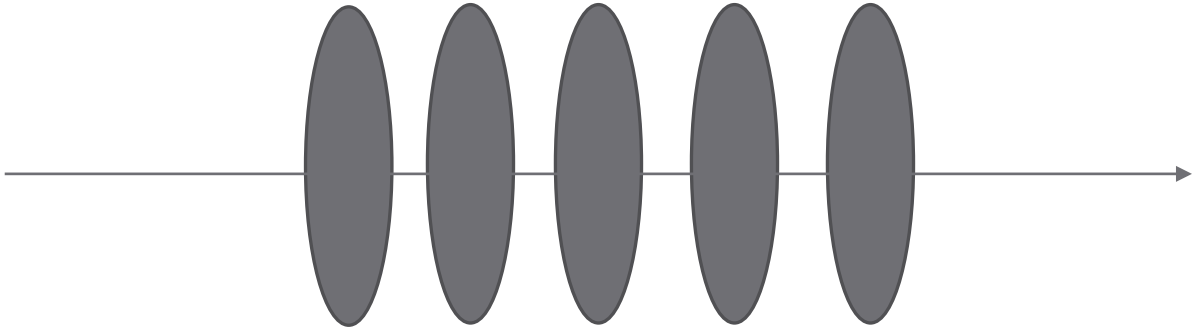

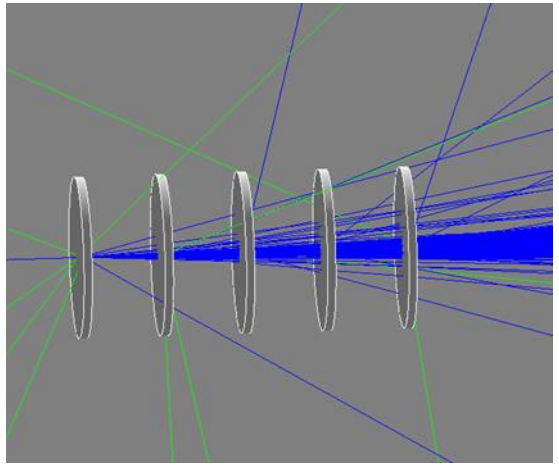

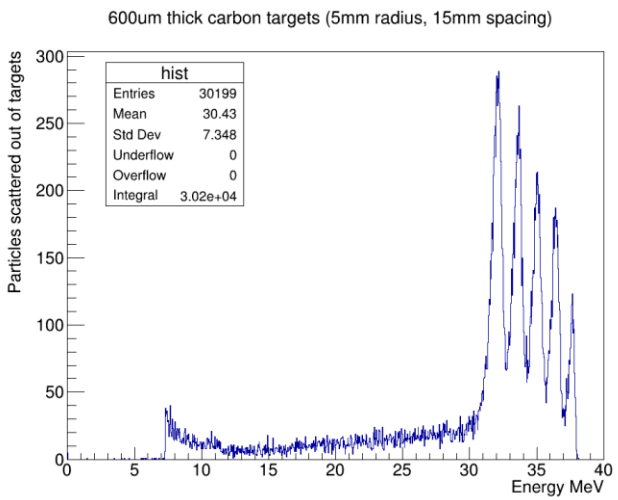
600um thick carbon targets (5mm radius, 15mm spacing)
Particles scattered out of targets
Energy MeV
hist
Entries 30199
Mean 30.43
Std Dev 7.348
Underflow 0
Overflow 0
Integral 3.02e+04

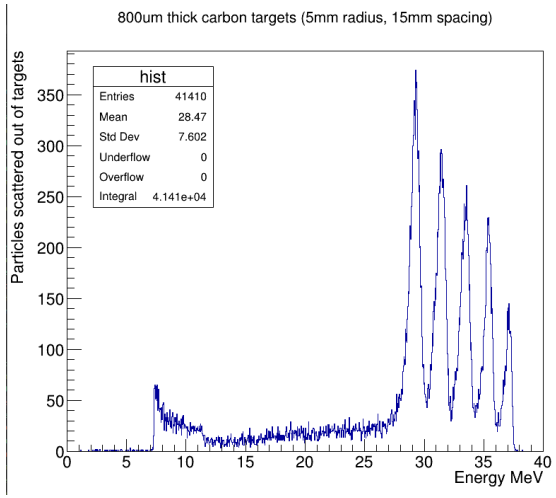
800um thick carbon targets (5mm radius, 15mm spacing)
Particles scattered out of targets
Energy MeV
hist
Entries 41410
Mean 28.47
Std Dev 7.602
Underflow 0
Overflow 0
Integral 4.141e+04

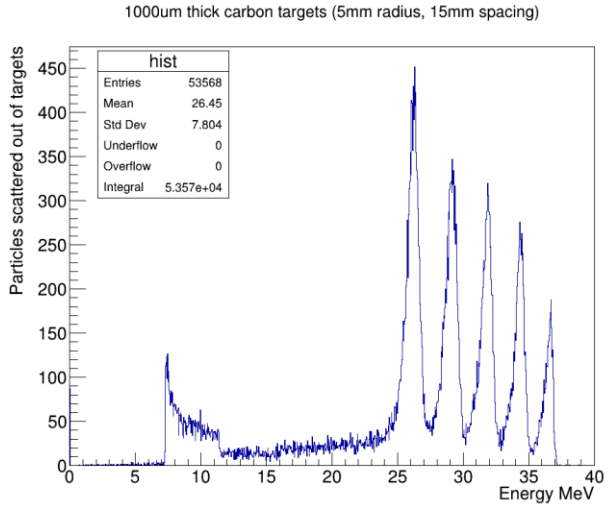
1000um thick carbon targets (5mm radius, 15mm spacing)
Particles scattered out of targets
Energy MeV
hist
Entries 53568
Mean 26.45
Std Dev 7.804
Underflow 0
Overflow 0
Integral 5.357e+04

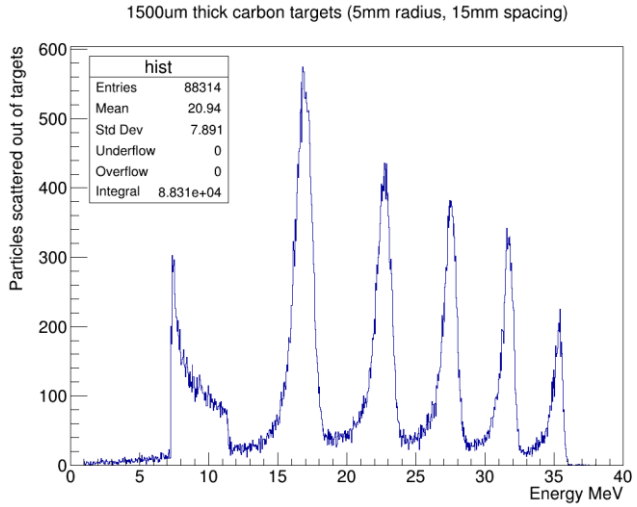
1500um thick carbon targets (5mm radius, 15mm spacing)
Particles scattered out of targets
Energy MeV
hist
Entries 88314
Mean 20.94
Std Dev 7.891
Underflow 0
Overflow 0
Integral 8.831e+04

Split Target Investigations

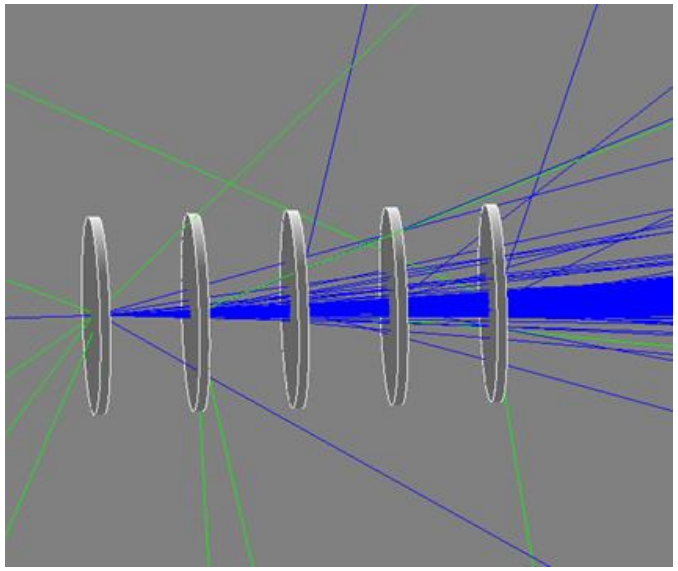

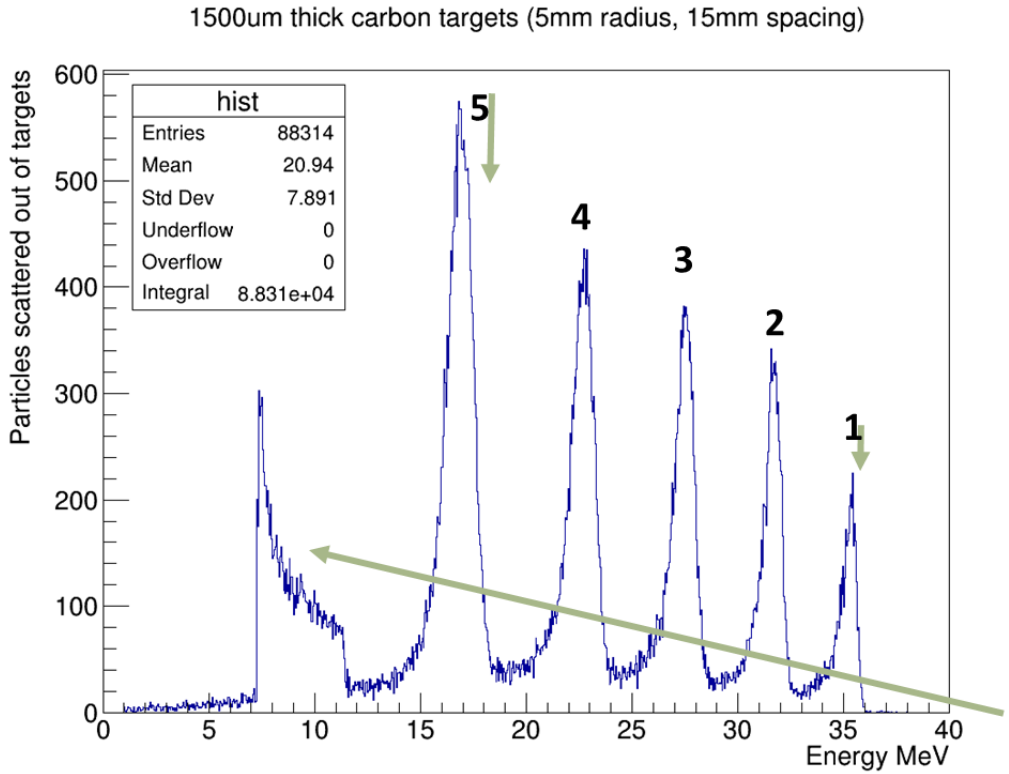

Scatter from last target

Scatter from first target

Inelastic landau region
(Proportional to thickness)
(Seems to be radius independent on first testing)

Carbon (Diamond) 45MeV

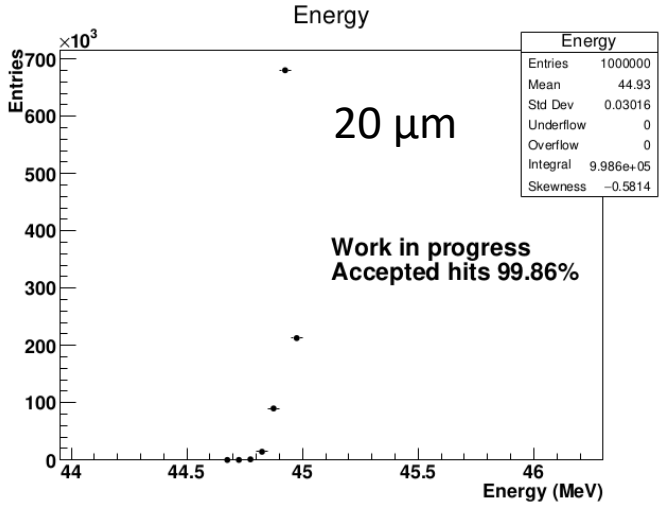

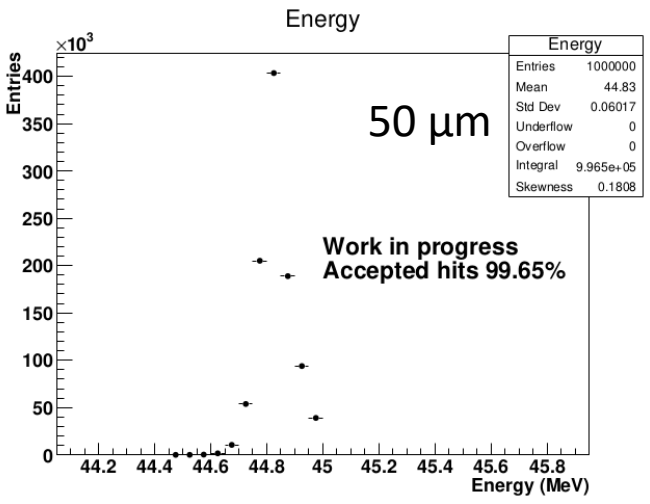

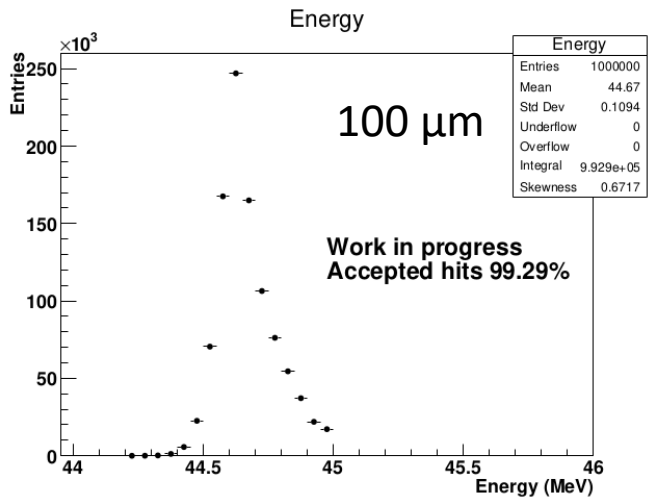

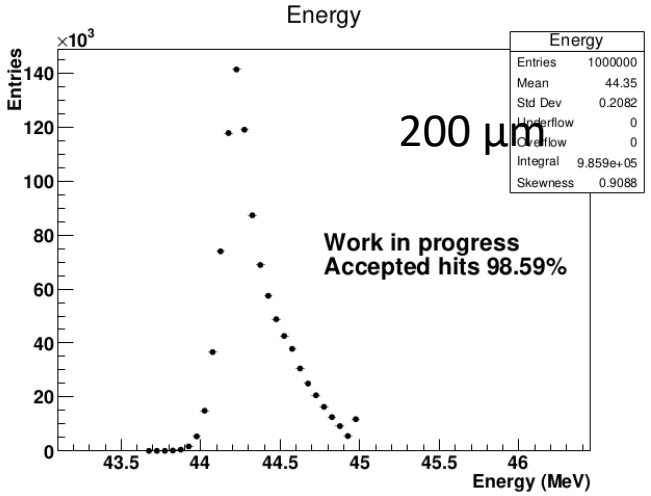

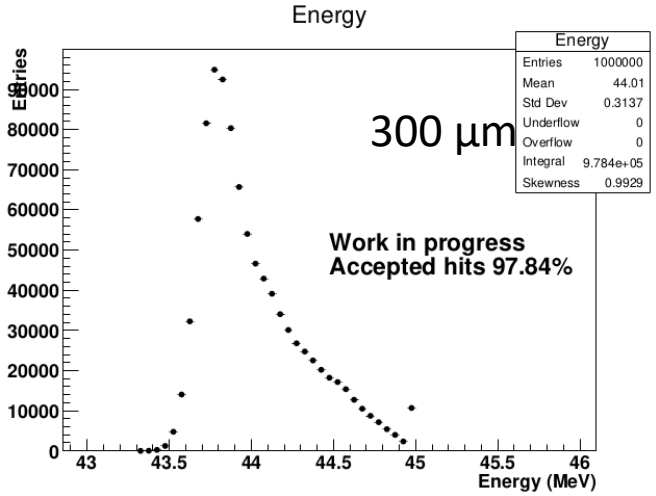

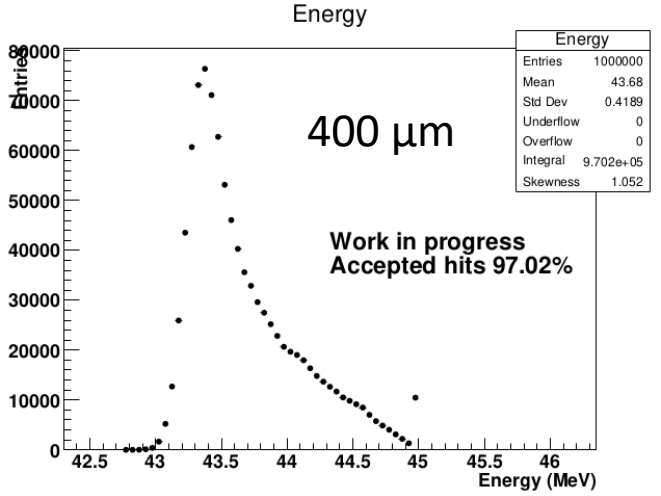

30 MeV

1° acceptance

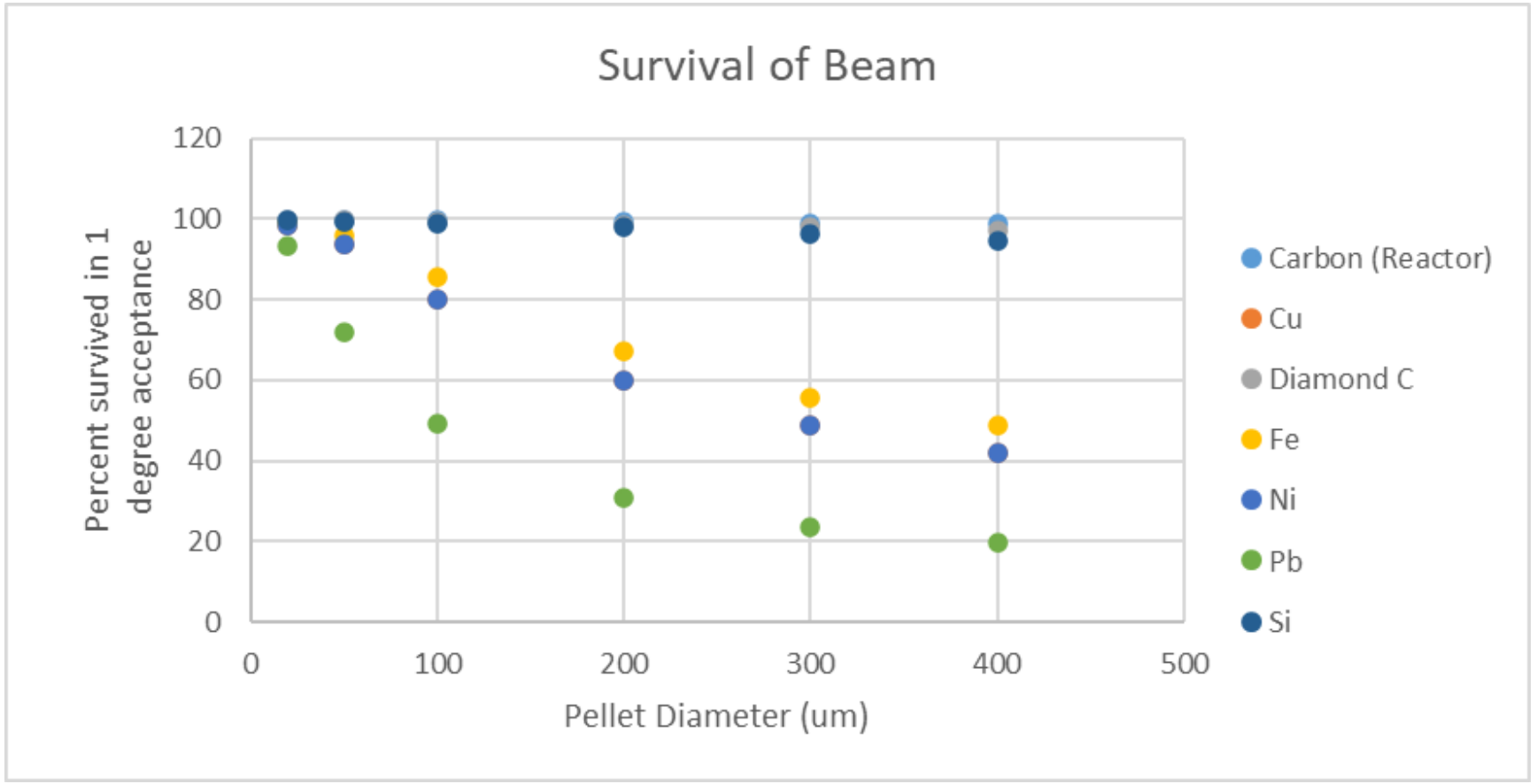

Beam defined as 1% larger diameter then pellet:
- 1.97% by definition passes pellet without interaction

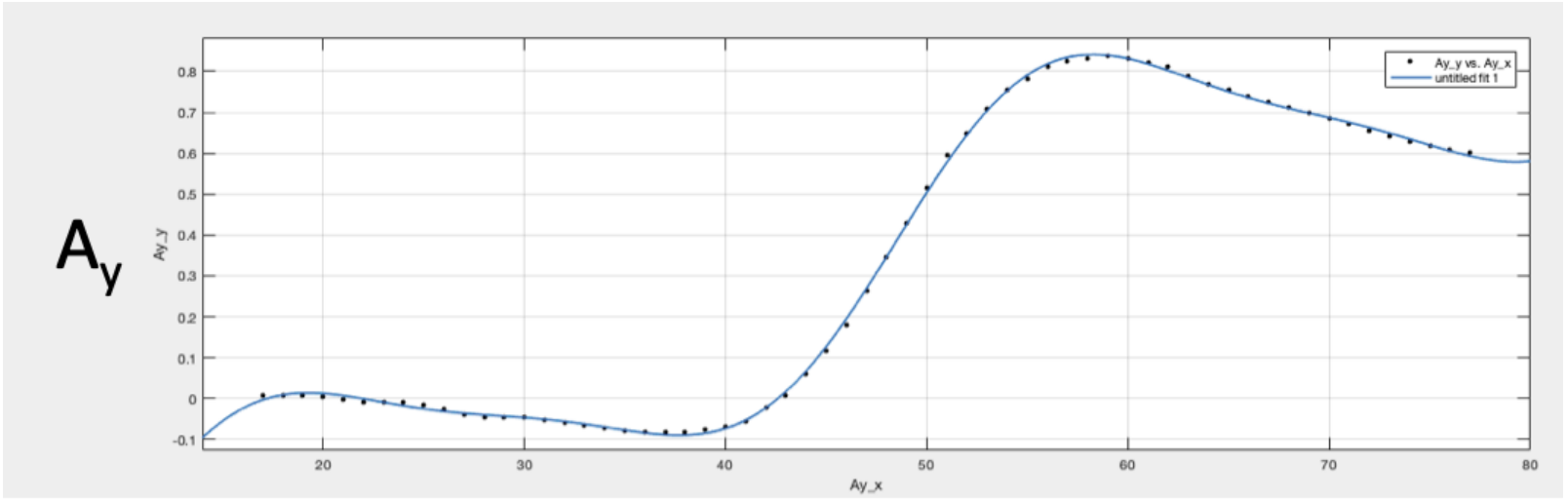
A_y
Ay_y vs. Ay_x
untitled fit 1
Ay_y
Ay_x
Angle (°)

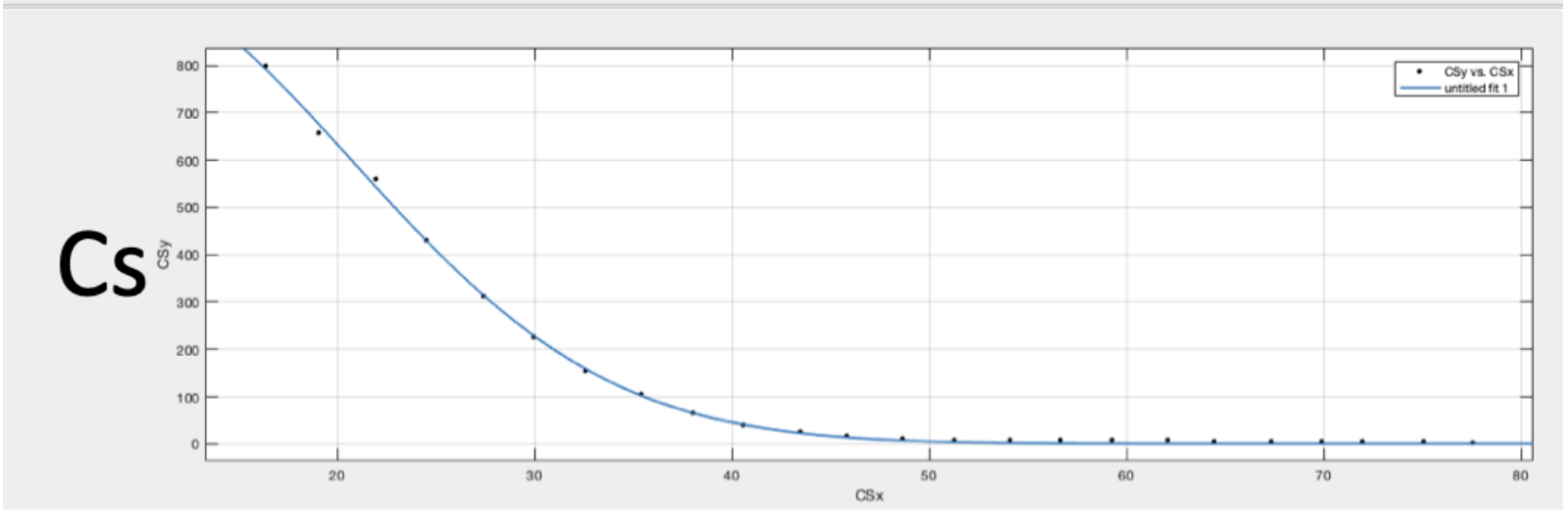
Cs
CSy vs. CSx
untitled fit 1
CSy
CSx
Angle (°)

39.6 MeV

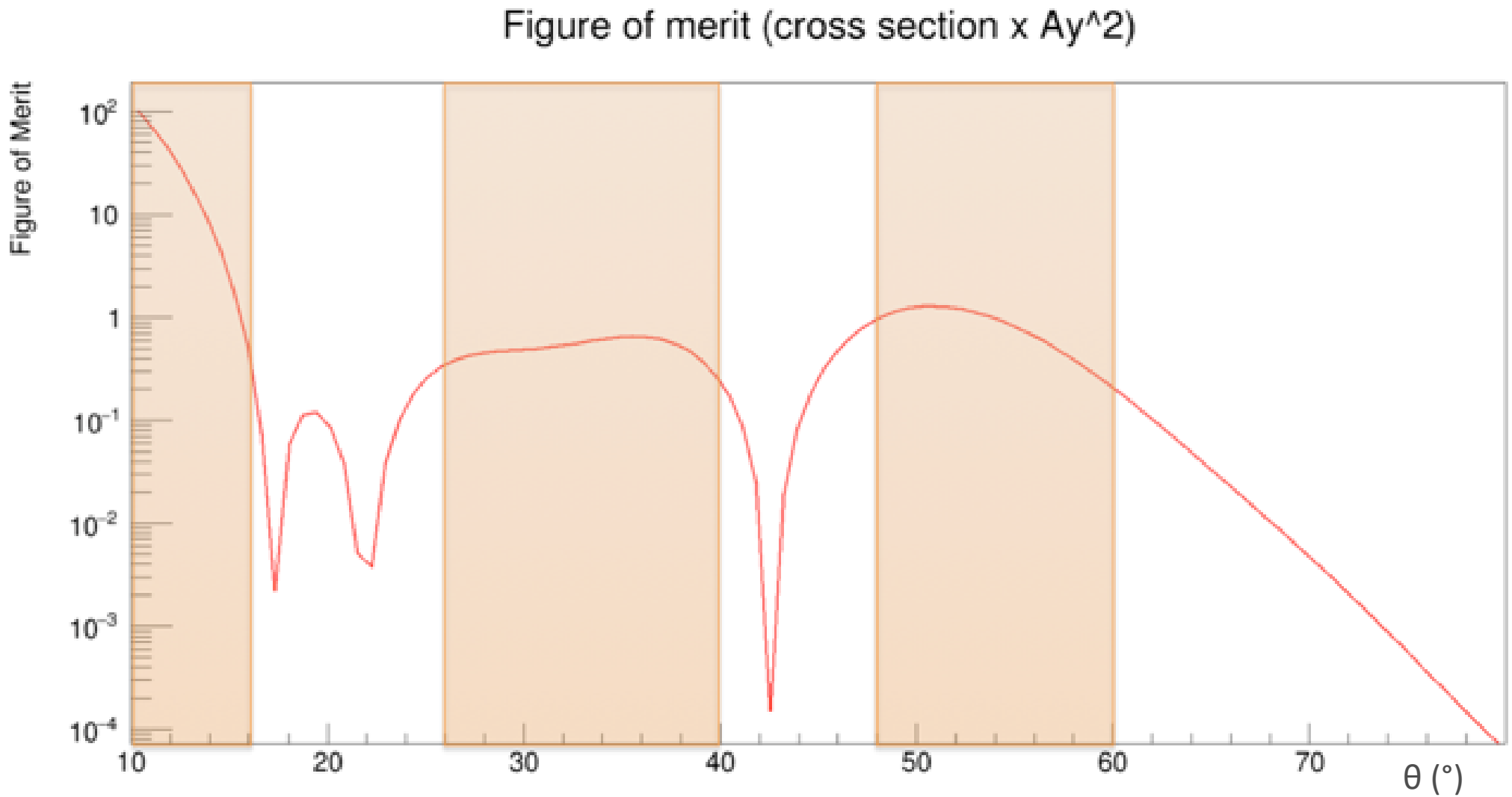
Figure of merit (cross section x Ay^2)
Figure of Merit
10^2
10
1
10^-1
10^-2
10^-3
10^-4
10
20
30
40
50
60
70
θ (°)

Price/performance	Due to industry standard processes, they are comparatively cheap for the performance when compared to conventional hybrid sensors.
Signal output	Due to in-pixel amplification and processing, the signal output from each pixel is very high and well digitized.
Signal/noise ratio	Low leakage current as well as in pixel amplification causes a high signal-to-noise ratio.
Fill factor (FF)	The readout electronics can be integrated in the sensing area of the pixels which leads to a fill factor close to 100\% although some components such as bias blocks, voltage regulators and I/O pads cannot be built into the sensitive area.
Time resolution	Good timing resolution, up to 5 ns after timing corrections has been achieved.
Radiation tolerance	Large depletion voltages can be used. This leads to fast collection of charge carries from the depleted area which causes the sensors to be less susceptible to radiation damage allowing radiation tolerance of 10^{15} $n_{eq}cm^{-2}$.

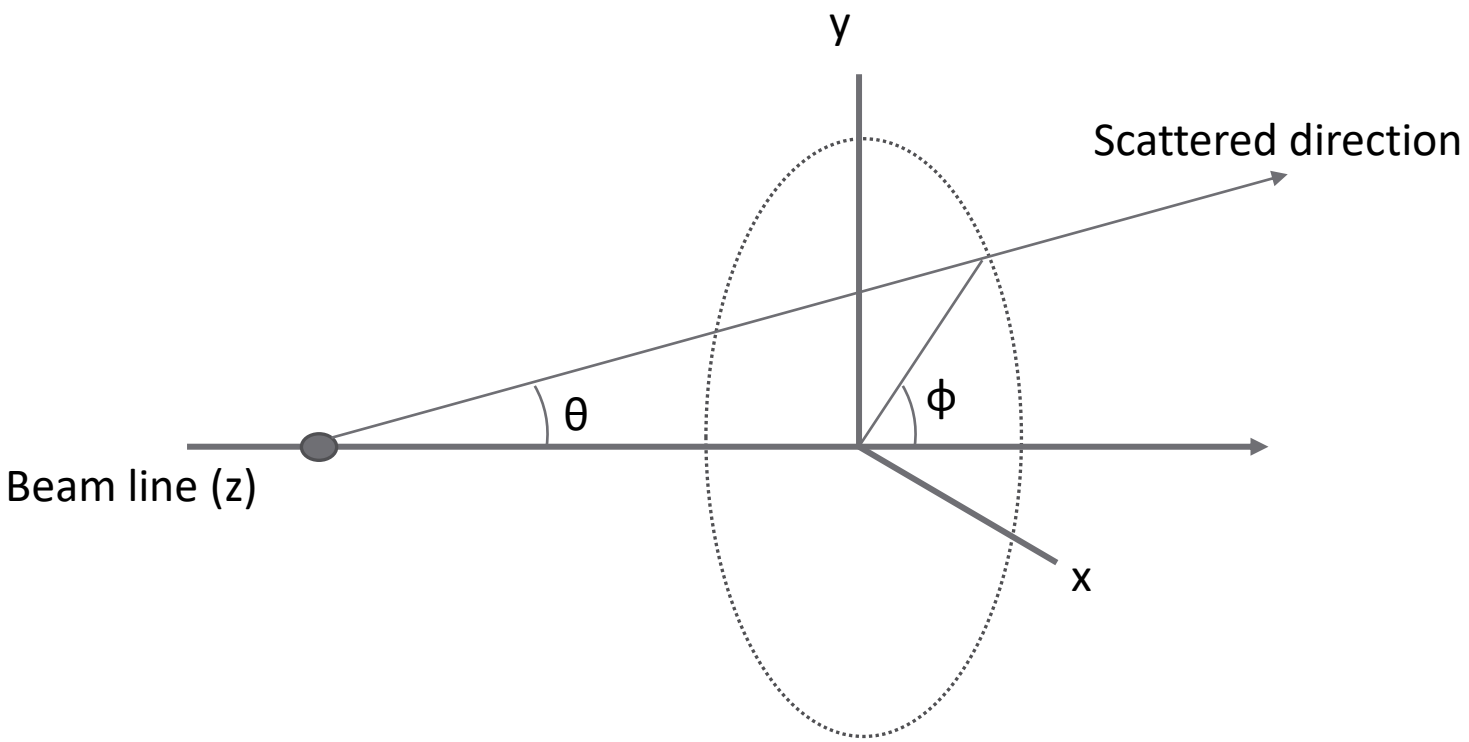
y
Scattered direction
θ
ϕ
Beam line (z)
x